What Atomistic Simulations Tell Us about Grain Evolution

SAND2013-3087C

Stephen M. Foiles
Sandia National Laboratories
Albuquerque, NM, USA

Collaborators:

- Elizabeth Holm, Carnegie-Mellon U.
- Garritt Tucker, SNL
- Eric Homer, Brigham Young University
- David Olmsted, University of California, Berkeley
- Greg Rohrer, Carnegie Mellon University
- Tony Rollett, Carnegie Mellon University

5th International Conference on Recrystallization and Grain Growth
Sydney, Australia
5 – 10 May, 2013

LDRD LABORATORY DIRECTED RESEARCH & DEVELOPMENT
U.S. DEPARTMENT OF ENERGY | Office of Science

Sandia National Laboratories is a multi-program laboratory managed and operated by Sandia Corporation, a wholly owned subsidiary of Lockheed Martin Corporation, for the U.S. Department of Energy's National Nuclear Security Administration under contract DE-AC04-94AL85000.

Sandia National Laboratories

Methods spanning orders of magnitude in length and time are employed to describe material response

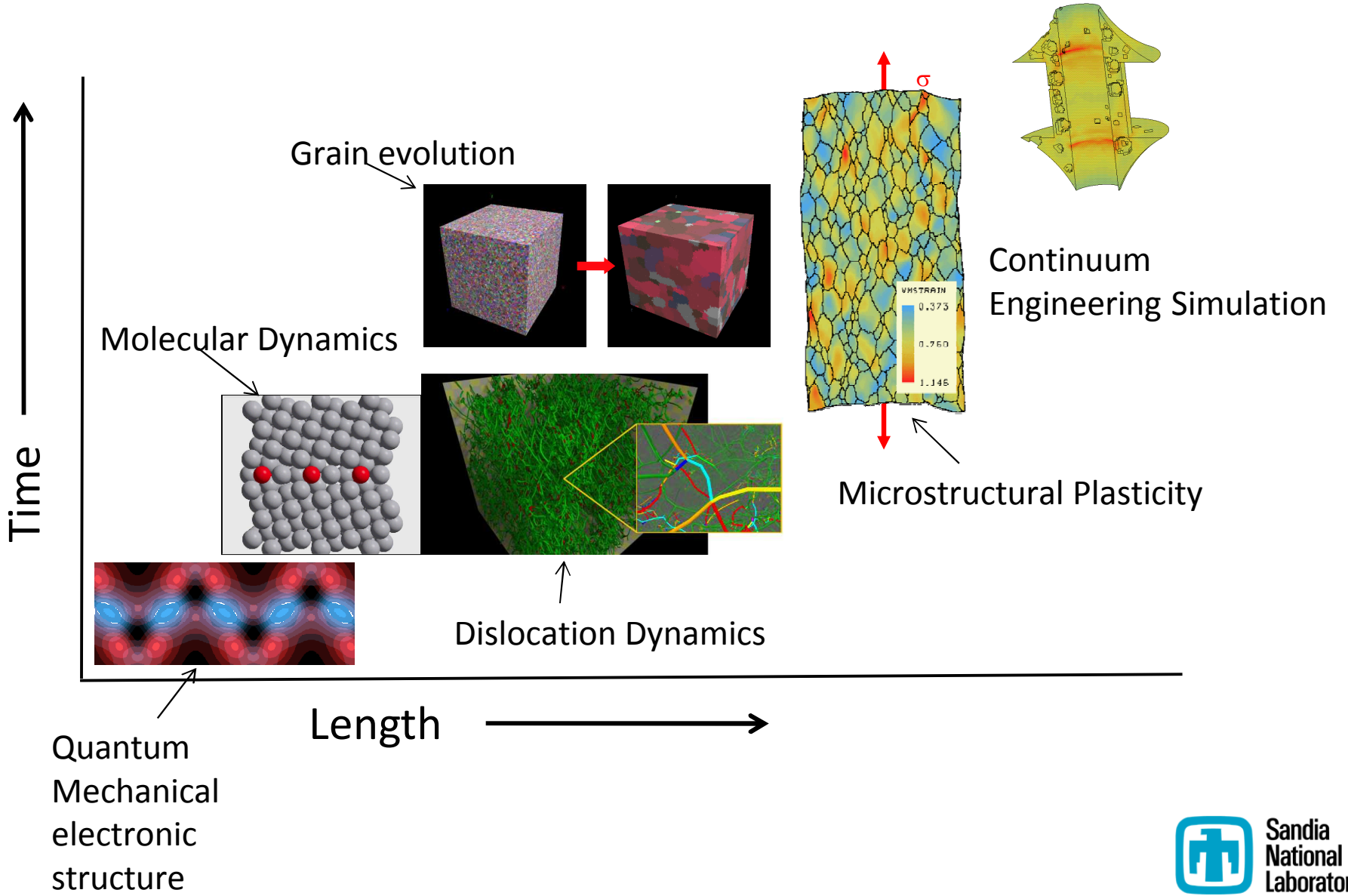

Sandia National Laboratories

Molecular Dynamics

- Follow the Newtonian dynamics of a set of atoms based on a force law
  - Force law (aka interatomic potential model) approximates the bonding due to the electronic degrees of freedom
    - In some cases, electronic structure calculations determine the forces, but typically it is a classical potential
- Primary challenges
  - Development of appropriate force law or interatomic potential
    - Must reproduce the dominant features of the bonding
    - Must be sufficiently computationally efficient to allow the problem of interest to be simulated
    - Not addressed in this talk
  - Problem definition and analysis
    - Must identify the key microscopic process to know what to simulate
    - Extracting understanding from the results
      - How does one turn millions of atomic coordinates into scientific insight?
    - Examples of doing this is the subject of this talk

Fundamental Limitation of MD

- Computational time limits the size and time scale that can be realistically simulated
  - Compute time scales linearly in both number of atoms (volume) and time
    - Limited by (Number of atoms)x(Time simulated)
  - A large but tractable simulation can currently treat up to ~1 atom-sec
    - Example: 20 million atoms for a time of 50 nanoseconds
  - This is many orders of magnitude smaller than a real world problem!
    - Cubic micron of material for 1 second: ~1011 atom-sec
    - Mole of material for a year: ~1031 atom-sec
- How can MD be relevant?
  - Multiscale modeling
    - Provide "information" needed by higher length scale models
      - Properties
      - Mechanistic insights
  - Fortuitous problems where the time and length scales of MD match the important processes

Outline

4 short case studies for microstructural evolution

- Pass information to meso-scale grain growth models
  - Grain Boundary Energies
    - Five-degrees of freedom challenge
    - Comparison with experimental observations
  - Grain Boundary Mobilities
    - Methodlogy
    - It is a lot more complicated than typically though
- Brute-force simulations of grain evolution
  - Annealing of nanocrystalline grain structure
    - Comparison of growth kinetics to conventional models
  - Nano-indentation of nanocrystalline metals
    - Deformation induces grain growth?
    - Identification of deformation mechanisms

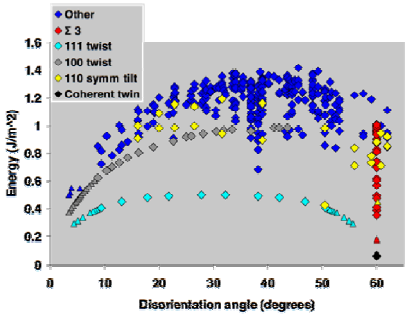

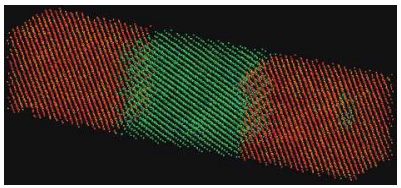

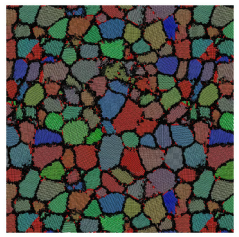

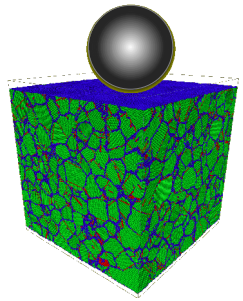

Sandia National Laboratories

Computational survey of grain boundary energies in FCC metals

- Using molecular statics, we built and minimized a catalog of 388 flat grain boundaries in Al, Au, Cu and Ni.
- Includes all boundaries that can fit inside a box of size 15a0/2.
- For each boundary, we minimize hundreds or thousands of configurations.
- Result: The largest computational survey of grain boundary energies.

- How do we use these results?
- Compare calculated energies with experimentally measured energies.
- Compare grain boundary energies in different FCC metals.

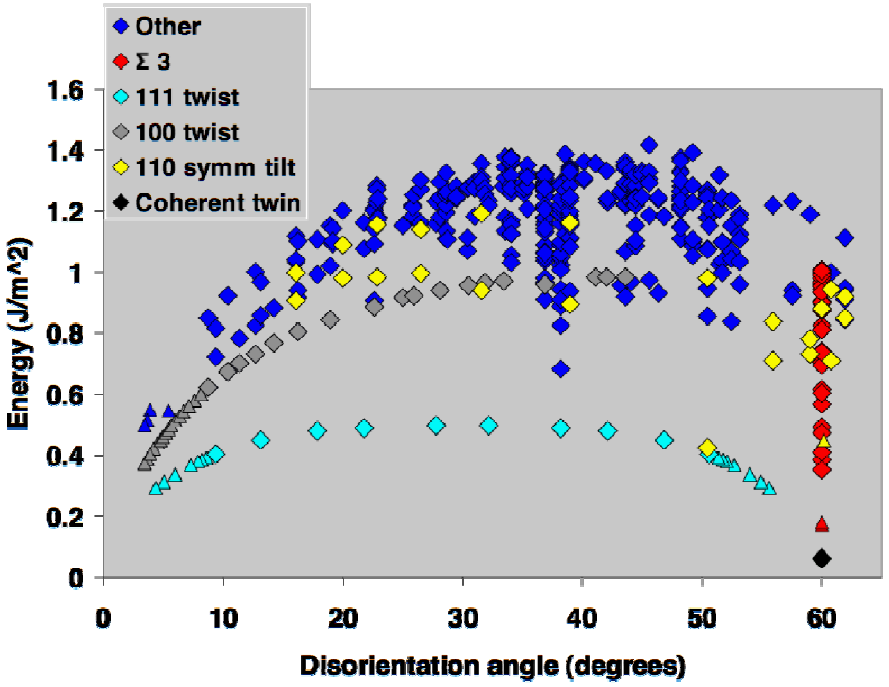

[Olmsted, Foiles, Holm, *Acta Mater.* **57** 3694 (2009)]

Sandia National Laboratories

Experimental measurement of grain boundary energies in Ni

- CMU used EBSD and serial sectioning to measure the relative energies of a large number of grain boundaries in Ni.
  - Measured 10^5 boundaries, binned into 17,894 bins (8.2° bin width).
  - 30% of boundaries are Σ3 type; 15% are Σ9 type.
  - 15% of bins contain < 5 measurements.

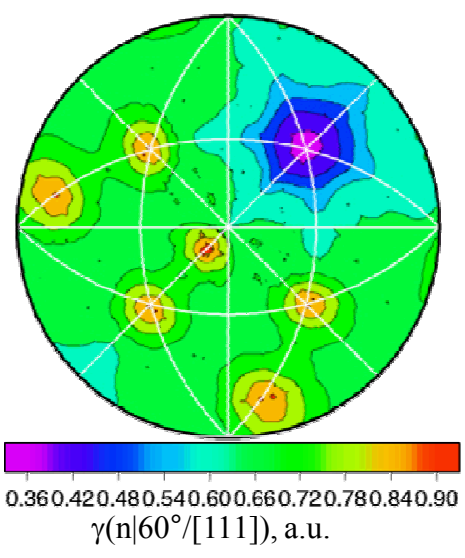

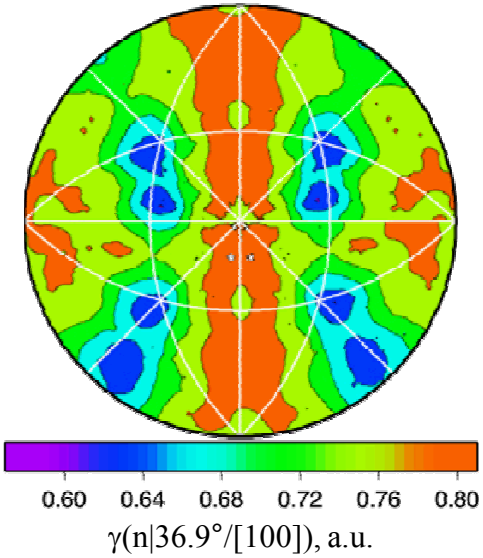

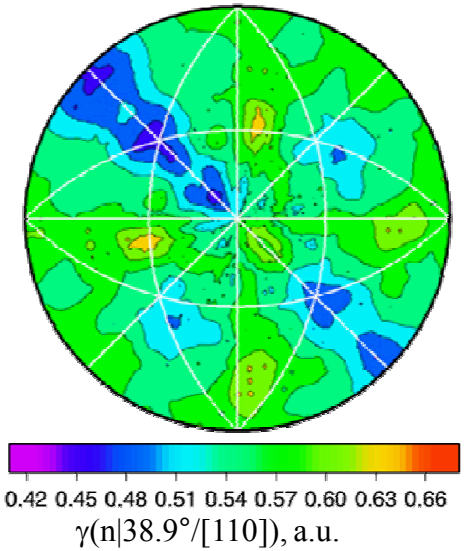

[Li, Dillon, Rohrer, *Acta Mater.* **57** 4304 (2009)]

Sandia National Laboratories

Comparing computation to experiment: unweighted correlation

- There is little correlation between measured and calculated grain boundary energies.
  - $R_U \sim 0.18$

Oh, No!
Calculations Wrong?!?

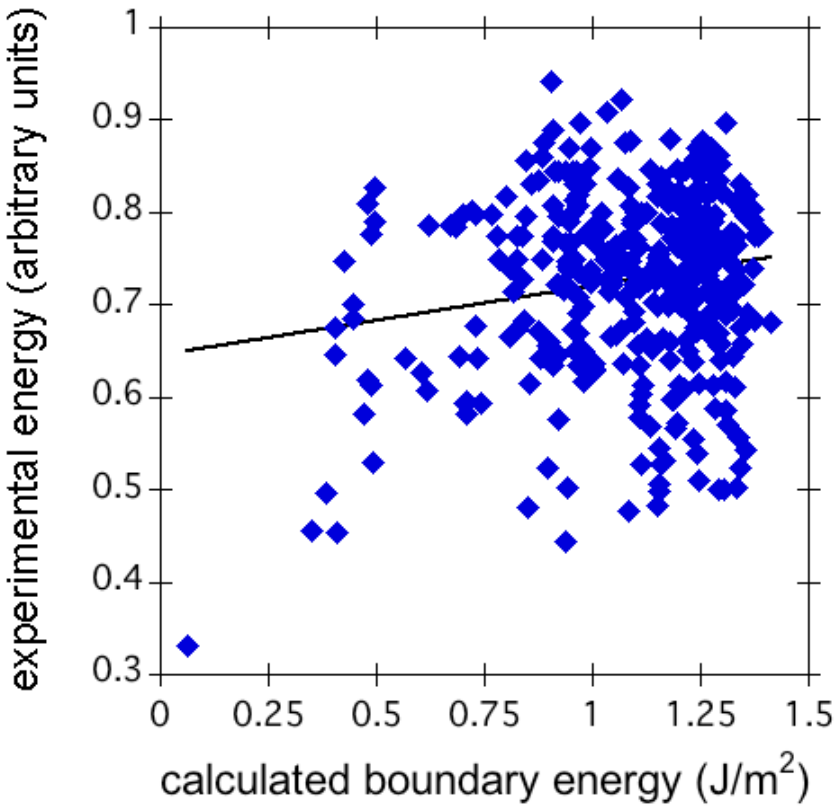

It must be the Experimental Analysis!

Sandia National Laboratories

Comparing computation to experiment: weighted correlation

- Energy bin population varies widely in the experimental data.
- When the correlation is weighted by the bin population, we find excellent agreement between experiment and simulation: $R_W \sim 0.92$.

⇒Experiments and simulations agree when the experimental statistics are adequate.

- For infrequently observed boundaries, the calculated energy is likely more accurate than the measured energy.
- Some frequently observed boundaries are rarely simulated; some infrequently observed boundaries are widely simulated.

⇒Experiments should guide selection of boundaries for simulation.

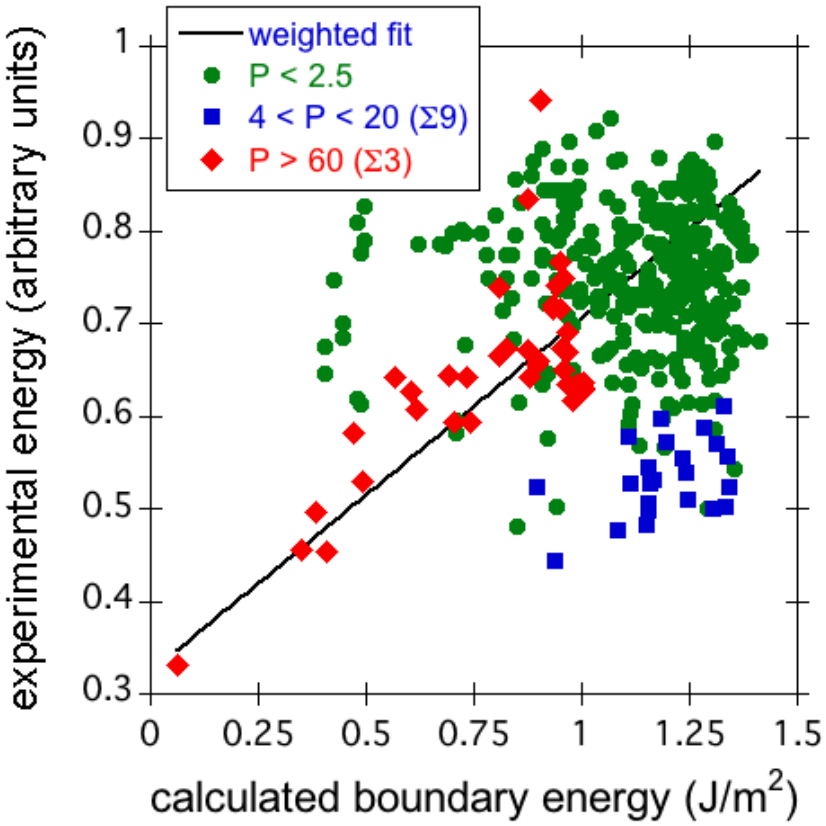

Sandia National Laboratories

Confirmation of Ni results: Boundary populations from an HEDM study

- High energy diffraction microscopy (HEDM) was used to assemble a large, 3D Ni grain structure:
  - Pure Ni, ~3500 grains, ~23,600 grain boundaries
- The measured GBCD shows excellent correlation with the calculated boundary energy for high population boundaries.

⇒This independent data set confirms the excellent agreement between experiment and simulation.

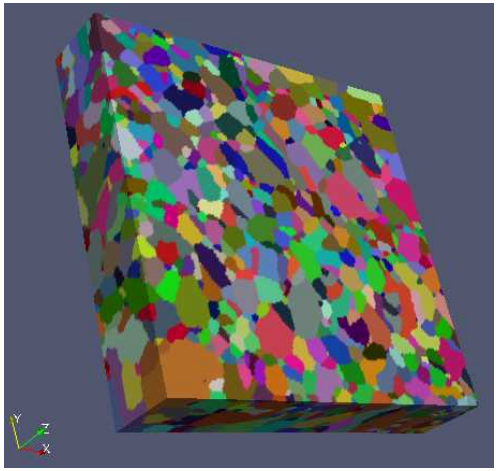

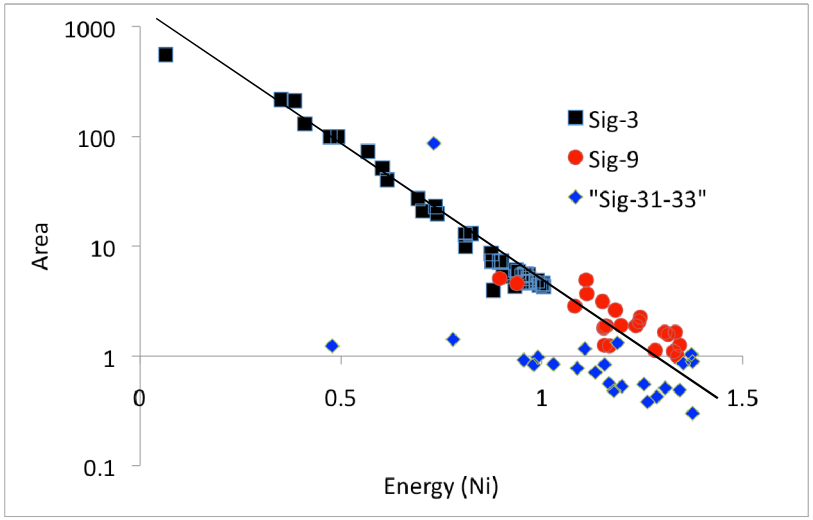

Sandia National Laboratories

In recent years, a variety of MD methods have been employed to compute boundary mobility

- Mobility relates the boundary velocity, v, to the driving force for boundary motion, "p"

$$v = Mp$$

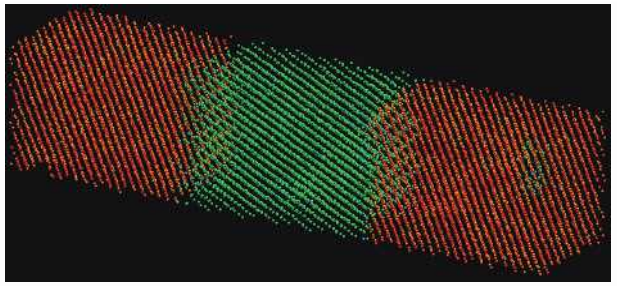

- Curvature driven methods
  - Exploit energy gain from reducing boundary area
- Stress driven boundary motion methods
  - Exploit anisotropic elastic constants to create energy density difference
- Synthetic driving force methods
  - Introduce an artificial energy that favors one grain
- Fluctuation methods
  - Consider boundary motion as a random walk and exploit the time-dependence of the fluctuations
- Hybrid synthetic and fluctuation methods

Boundary mobility calculated for a catalogue of 388 boundaries using a synthetic driving force method

[Janssens, Olmsted, Holm, Foiles, Plimpton and Derlet, Nature Materials 5, 124 (2006)]

- Apply a synthetic driving force for boundary motion:

For an atom in the favored/growing grain:	For an atom in the unfavored/shrinking grain:
$\varphi = \varphi_{EAM}$	$\varphi = \varphi_{EAM} + u$

- Excess potential energy function
  - Depends on position of an atoms neighbors
  - Zero in one grain, positive in another
- Now just run molecular dynamics with this addition energy term
  - Implemented in Sandia LAMMPS code for massively parallel MD (http://lammps.sandia.gov)

Additional free energy per atom drives the unfavored grain to shrink; thus the boundary moves. This energy is of undetermined, arbitrary origin.

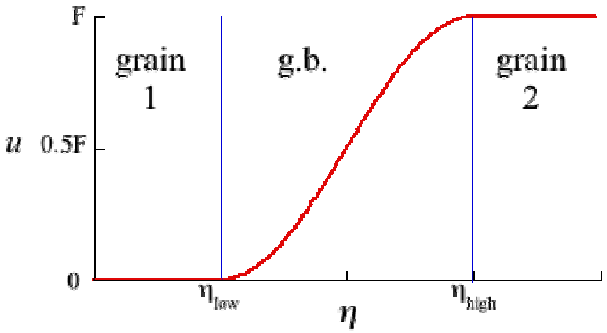

$$\eta_i = \sum_j \left| \left(\vec{r}_j - \vec{r}_i \right) - \vec{R}_{nn,j} \right|$$

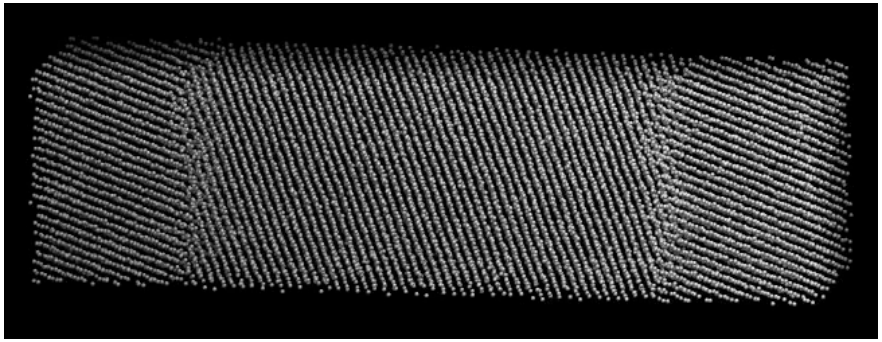

Mobility computed with artificial driving force agrees with calculations using elastic strain energy driving force where both methods can be applied.

Sandia National Laboratories

Grain boundary mobility vs. misorientation

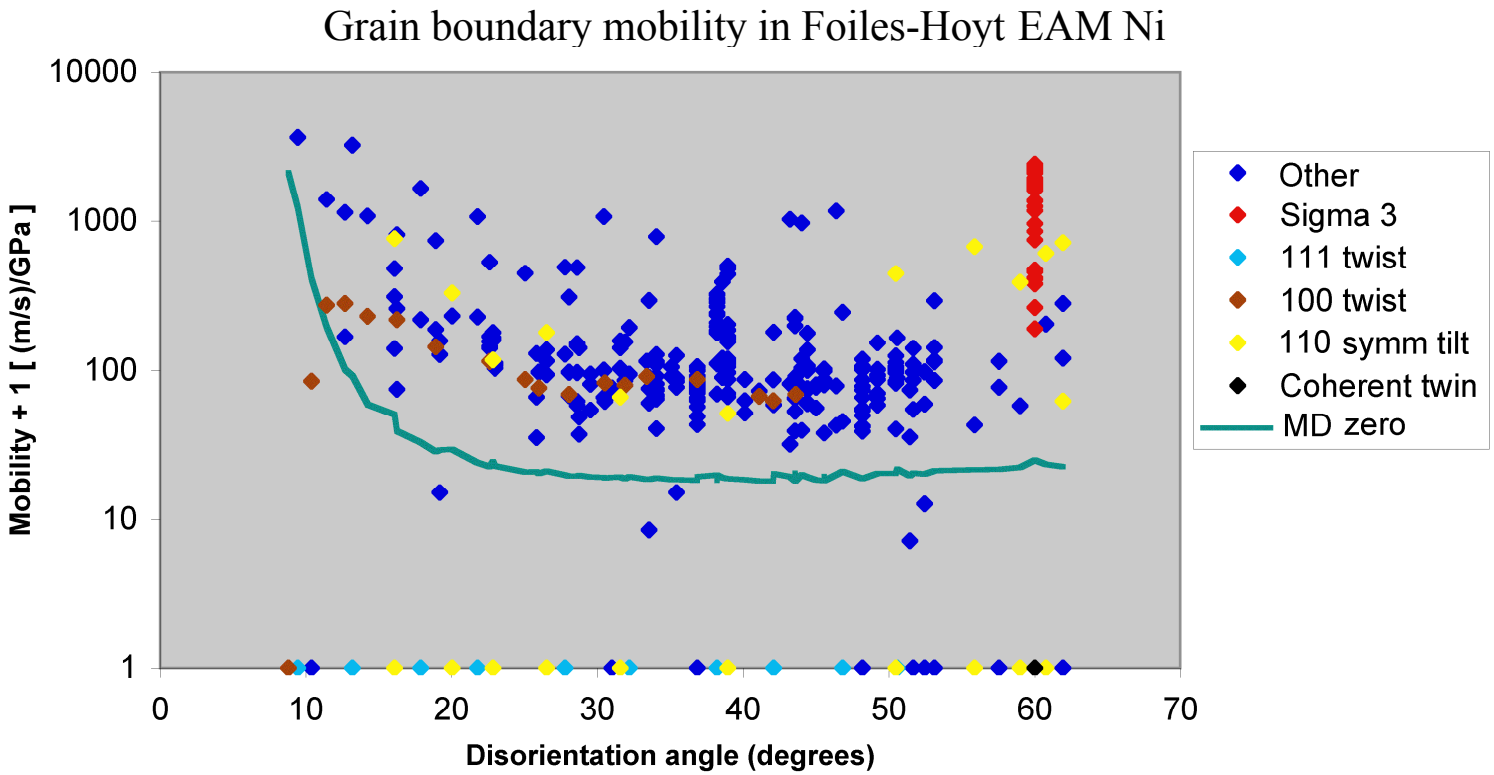

- Note the wide range of observed mobilities (log scale). Most have mobility around 100 m/s_GPa, but some are as high as 5000 m/s_GPa, or as low as 0 m/s_GPa.
- Mobility is not correlated with disorientation angle or boundary type, except <111> twist boundaries have very low mobility, as do some <110> symmetric tilts.
- The highest mobility boundaries are: Σ111 (9°), Σ57 (13°), and Σ3 (60°).

Sandia National Laboratories

Grain boundary mobility vs. temperature
Not as simple as we thought!

- Conventional wisdom presented in the standard textbooks is that grain boundary motion is an activated process

$$M = M_0 e^{-Q/kT}$$

- In a recent survey of grain boundary mobilities, we identified several classes of the temperature dependence of mobility
  - The majority of boundaries are thermally activated, and are slow at low temperatures
    - Roughening transitions often lead to especially slow motion at low temperatures
  - About 20% of boundaries are not thermally activated, and are fast at low temperatures
- **Understanding how boundary mobility varies with temperature is a topic of current research**

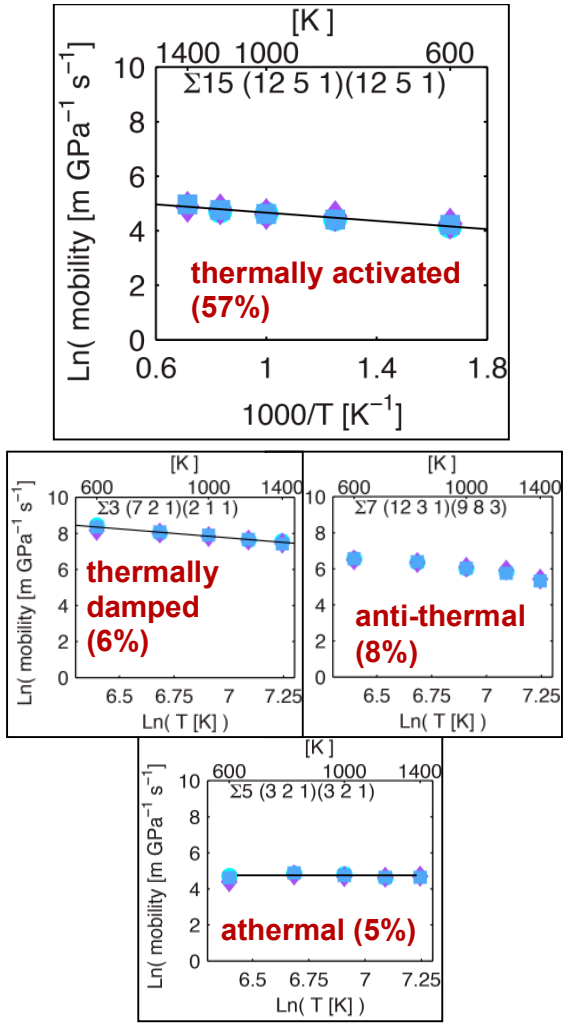

Olmsted, Foiles, Holm, *Acta Mater.* **57** (2009) 3704.

Sandia National Laboratories

Synthetic driving force MD confirms the existence of shear-coupled grain boundary motion

- Previous studies have shown that shearing certain grain boundaries induces boundary motion
  - Mostly studied for symmetric tilt boundaries
    - Cahn, Mishin, Suzuki, Acta Mater 54, 4953 (2006)
- Current work shows that driving boundary motion can induce shear
  - Coupling factors agree between methods
- Observations
  - Shear-coupling is observed for many boundaries that are not tilt boundaries
  - Boundaries that shear-couple have generally higher mobilities
    - If shear is prevented, these boundaries still move but with lower mobilities
  - Shear-coupling behavior can change with temperature

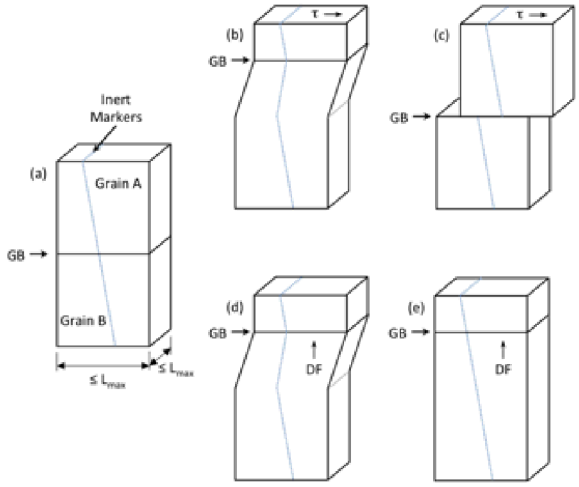

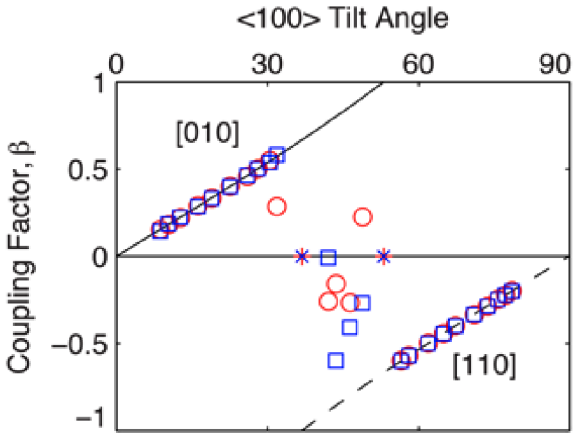

Homer, Foiles, Holm, Olmsted, Acta Materialia 61, 1048 (2013)

Sandia National Laboratories

Direct MD Simulation of Annealing of Nanograined Ni

- 3-D Cubic cell with periodic boundary conditions
  - Perform Isothermal-Isobaric dynamic
- Initial structure
  - Randomly centered and oriented grains
  - Voronoi construction of grains
    - Initial triple junction angles wrong
  - Typical initial grain diameter: ~5 nm
- EAM Potential for Ni

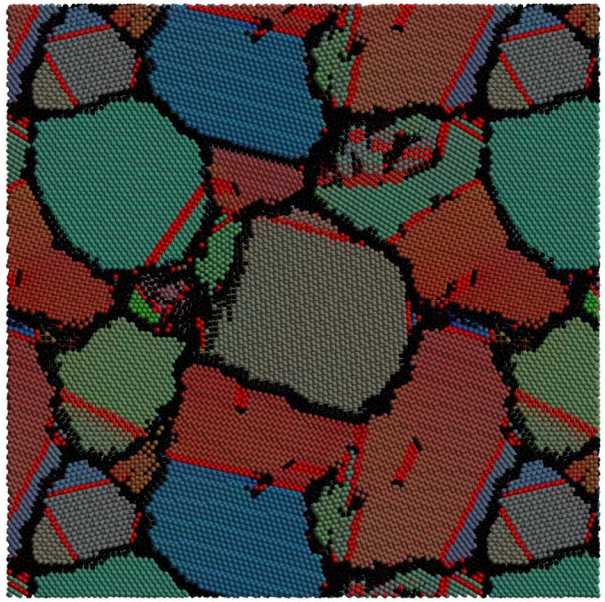

T/T_M	0.65	0.75	0.85
Cell side	19.5 nm	39.0 nm	39.0 nm
Initial Grains	100	800	800
# of atoms	~653,000	~5,104,000	~5,104,000
Time	10 ns	7 ns	2 ns

Sandia National Laboratories

Analysis identifies local grain orientation, twin and stacking faults, and boundaries

- For each atom, find the rotation that gives the best match between the locations of an ideal FCC first neighbor shell and the actual neighbors of the atom
  - If good match, FCC environment and rotation defines local crystal orientation
    - Color the atom based on the orientation
  - If poor match, repeat for an ideal HCP first neighbor shell
    - If good match, atom is locally in HCP environment
      - Color the atom RED
  - If neighbors don't match either FCC or HCP
    - Atom in a locally disordered region
      - Here they are mostly grain boundary atoms
    - Color the atom BLACK
- This produces the images
  - Show slices through the 3D cell

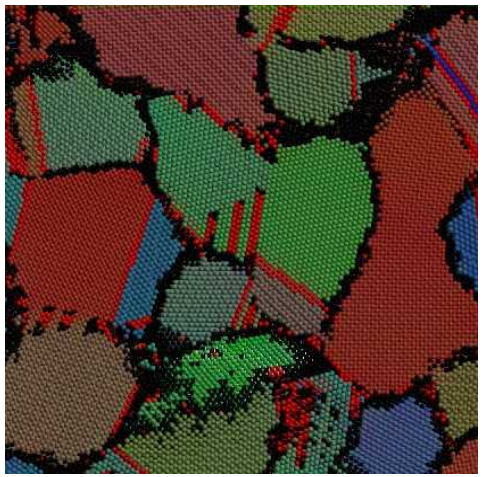

Sandia National Laboratories

Visualization of Grain Growth at T = 0.75 T_M

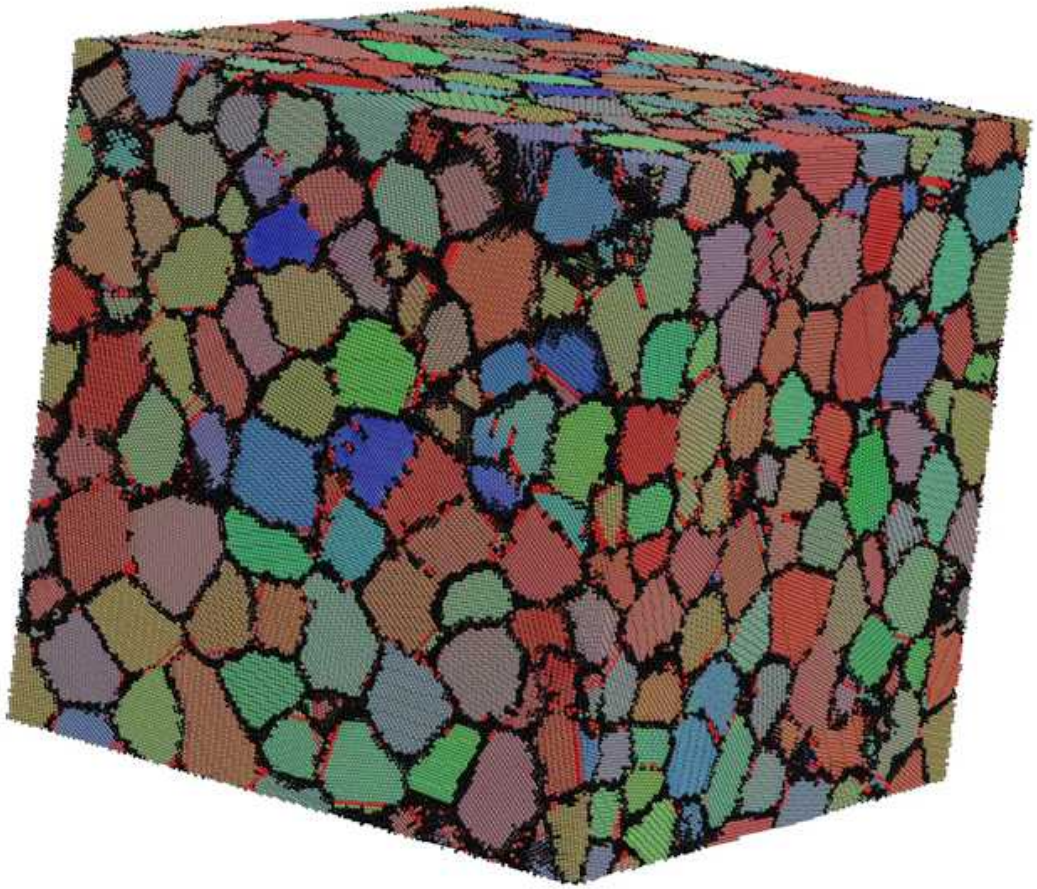

Sandia National Laboratories

Brute Force MD can follow grain growth in nanocrystals
What do we learn?

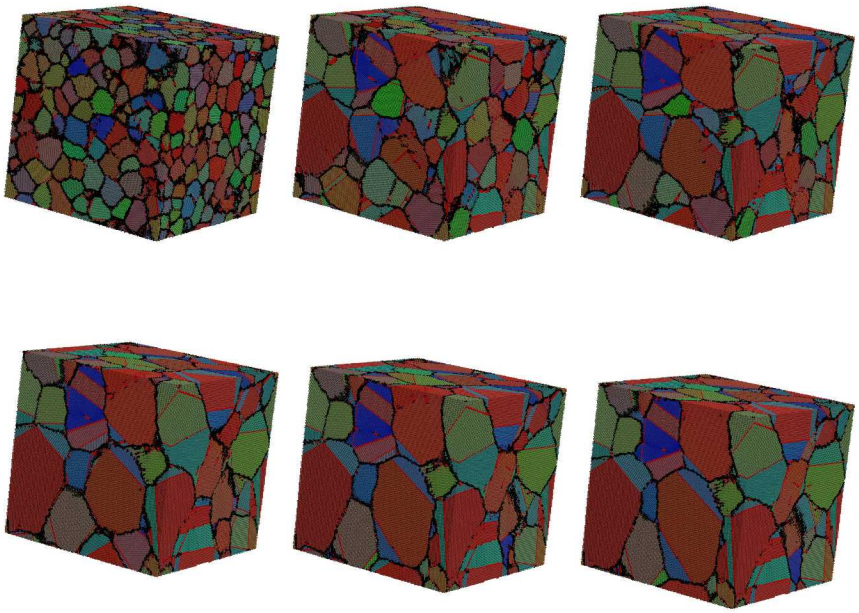

T = 0.75 T_M; 39 nm cube;
1.0 ns steps

- **Formation of twin boundaries**
- **Vacancies seen in grain interior**

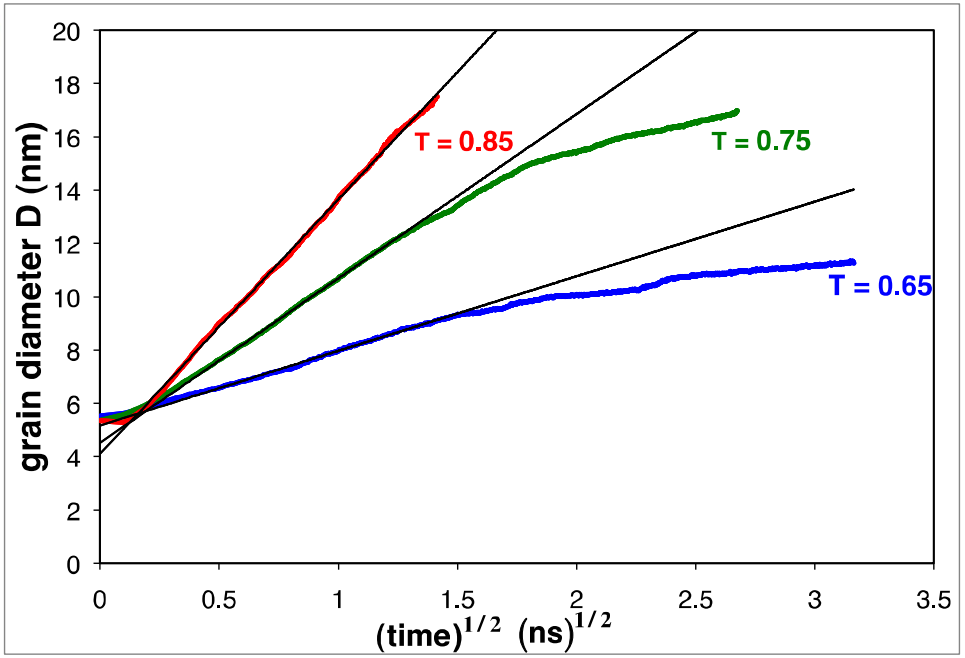

- **Initial transient is not physical**
- **Conventional scaling of grain size with time$^{1/2}$ observed for significant period**
- **Why does the growth slow down?!?**

Sandia National Laboratories

MD simulations can study individual boundaries: Catalog of mobility for 388 Ni grain boundaries

How could one use such data?

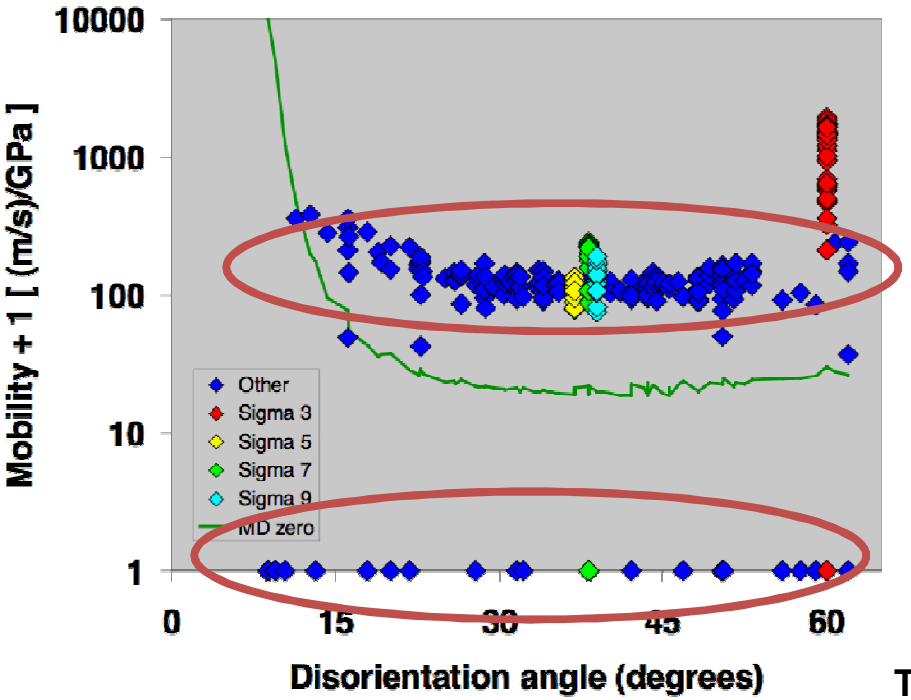

Can consider crystallographic dependence of mobility.

-But no trends in M found

-But not enough data to interpolate

Can look for groups of similar boundaries, regardless of crystallography

-High mobility boundaries

-Low mobility boundaries

- **Relative fraction of High and Low mobility boundaries is temperature dependent**
- **In many boundaries, associated with roughening**

Transition temperature between low/high mobility

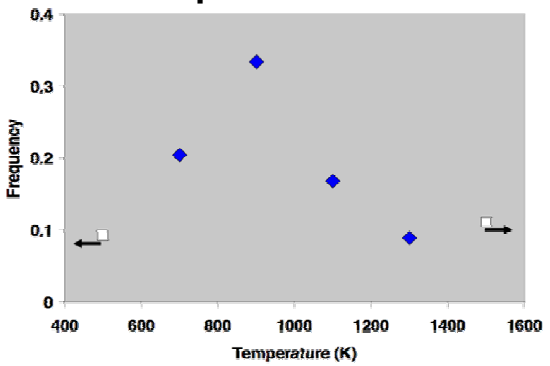

Sandia National Laboratories

Mesoscale Microstructure Simulations reveal the consequences of temperature dependent population of High/Low mobility boundaries

- Monte Carlo Potts Model simulations
  - Low mobility: $M \sim 0$
  - High Mobility: $M \sim 1$
  - Fraction, f_0, of High/Low mobility
  - Allow system to evolve via normal grain growth physics

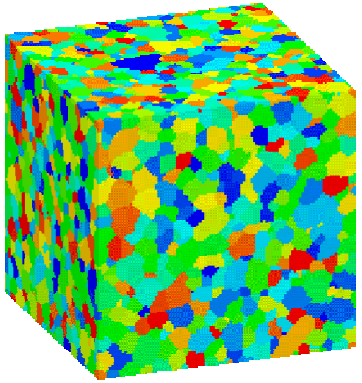

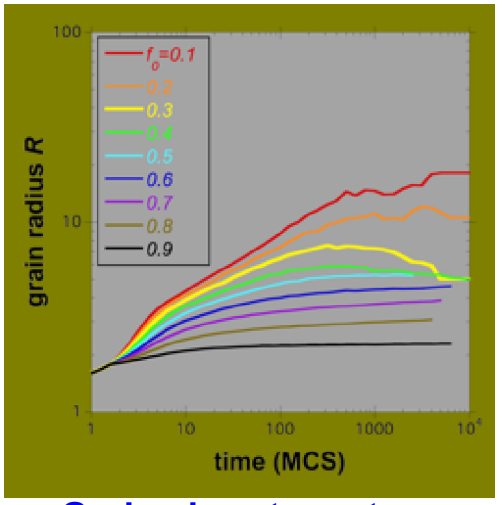

- Grain size stagnates
- f_0 determines final size

T (K)	f_0
600	0.9
800	0.7
1000	0.35
1200	0.2
1400	0.1

Convert temperature to fraction of low mobility boundaries

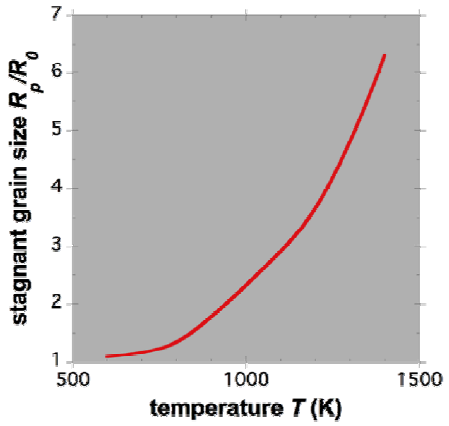

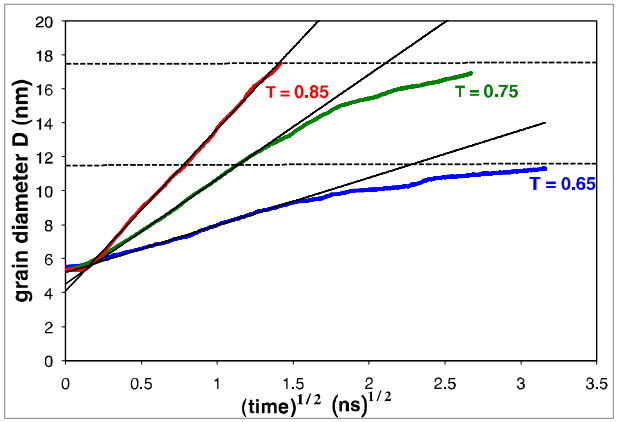

Explanation of grain growth stagnation in pure metals?
Holm, Foiles, Science 328, 1138 (2010)

Sandia National Laboratories

Mechanically-induced grain growth limits the fatigue life of nanocrystalline metals.

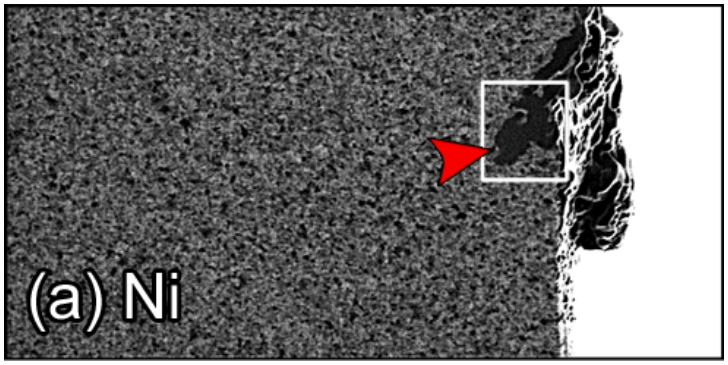

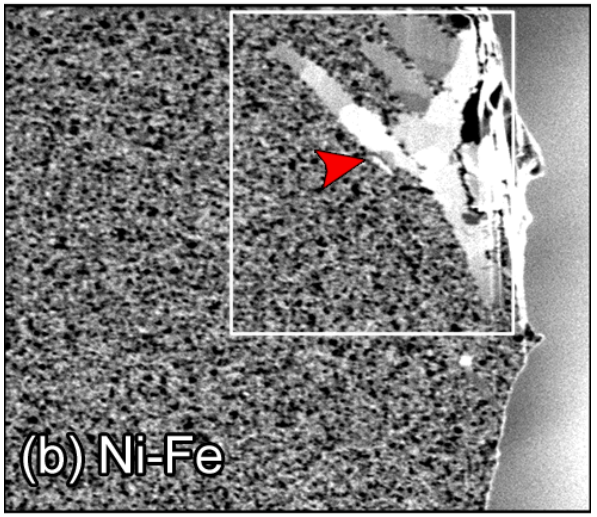

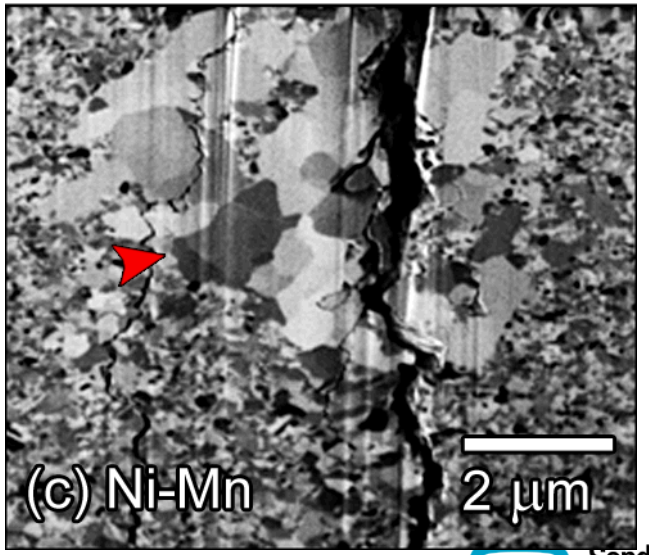

- During fatigue tests of nanocrystalline alloys, failure is always observed to initiate at colonies of very large grains.
- These abnormal grains develop during fatigue testing.
  - Room temperature
  - Nominally elastic
  - High Schmid factor grains
- In the absence of large grains, the material does not fail.

Boyce and Padilla, *Metall. Mater. Trans A* **42A** (2011) 1793.

Sandia National Laboratories

Mechanically induced grain growth – over a wide temperature range - has been recognized for decades

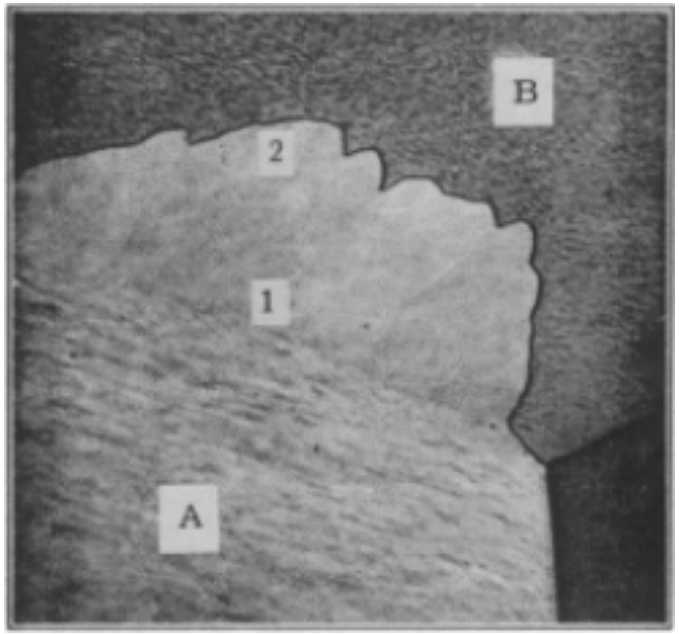

Plastic strain-induced boundary migration in deformed Al, observed during annealing at 350°C.

- Driving force is direct removal of stored dislocations by boundary sweeping.

Beck and Sperry, *J. Appl. Phys.* **21** (1950) 150.

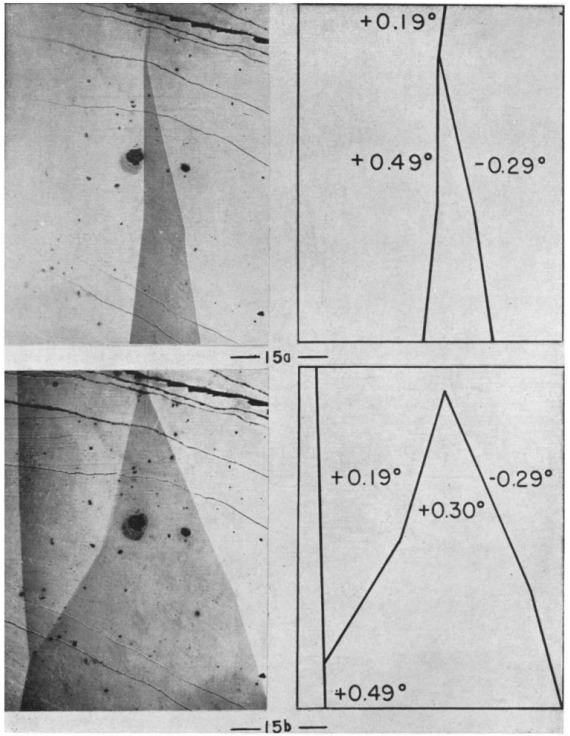

Elastic stress-induced, reversible low-angle grain boundary migration in Zn bicrystals at -196°C and 375°C.

- Driving force is relief of elastic stress via grain boundary dislocation motion.

Bainbridge, Li, and Edwards, *Acta Metall.* **2** (1954) 322.

Sandia National Laboratories

Increases in mechanically-induced grain growth have been observed as temperature decreases.

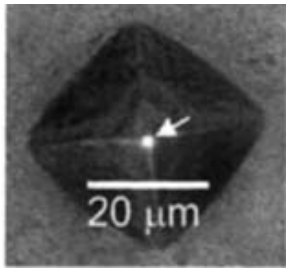

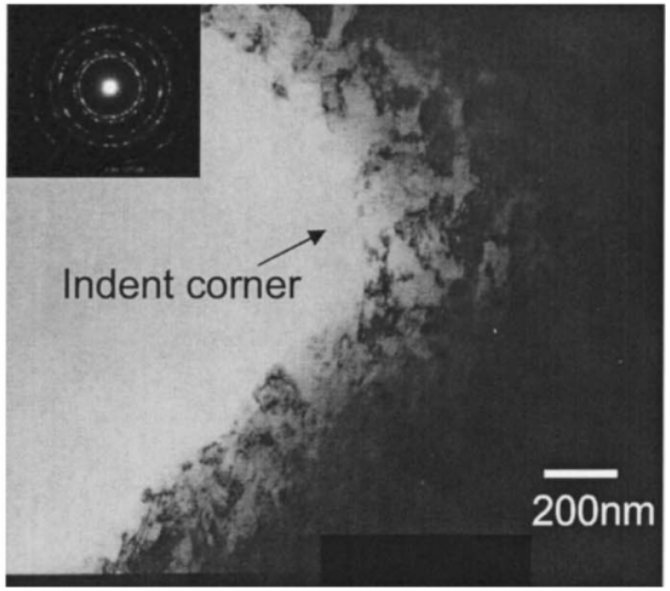

In indentation studies of nanocrystalline Cu, grain growth was more extensive at cryogenic (LN_2) temperatures than at room temperature.

- Growth was most prominent near the indent corner, i.e. in the highest strain region.

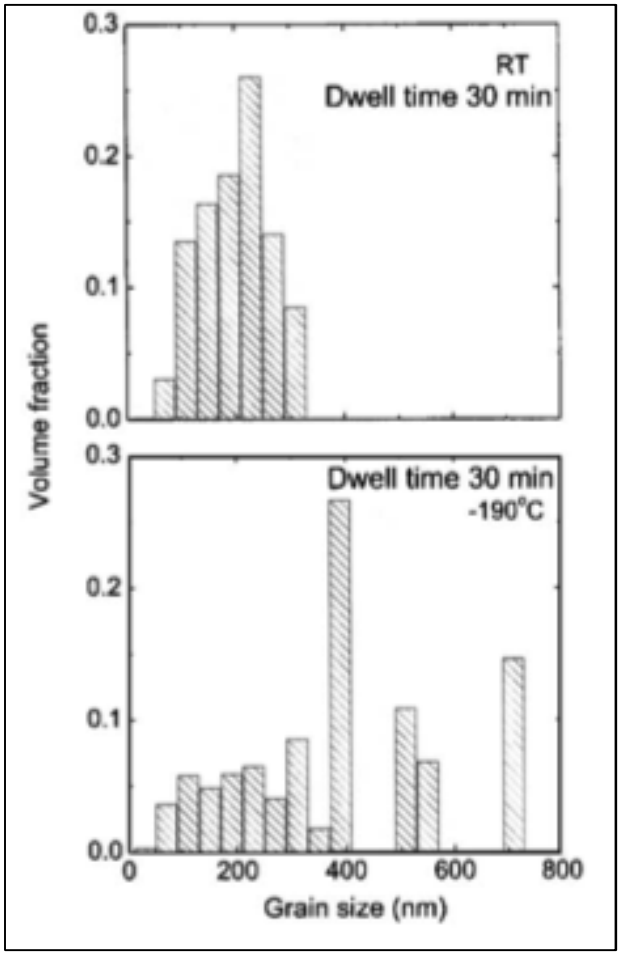

Zhang, Weertman, and Eastman, *Appl. Phys. Lett.* **87** (2005) 061921.

Sandia National Laboratories

Computational Methodology – Initial State

- Thin film (X/Y periodicity, free surface in Z)
- 3D Voronoi Tessellation
  - ~4nm grain size
  - Random orientations
- Thermal equilibration at 1175 K (0.75 T_m) for 0.2 ns
  - Thermal grain growth leads to about half the number of grains and equilibrates triple junctions
- Ni EAM potential (Foiles et al. 2006)
- a_o adjusted for thermal expansion
- Thermal equilibration at 300K for 0.05 ns

→ $(53\ nm)^3$ containing about 13 million atoms

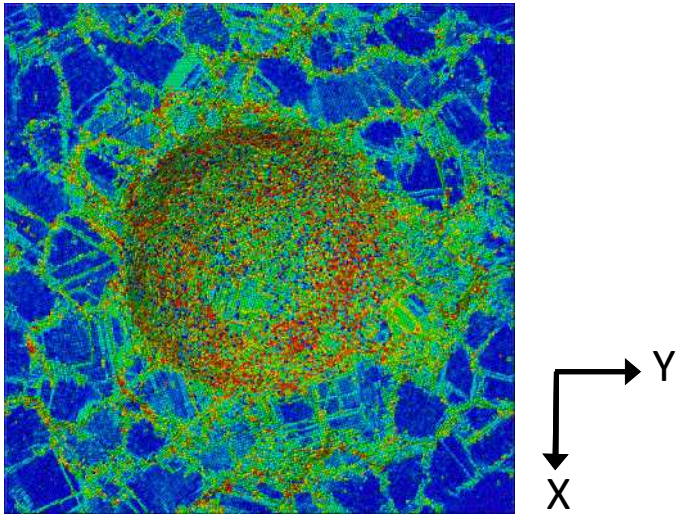

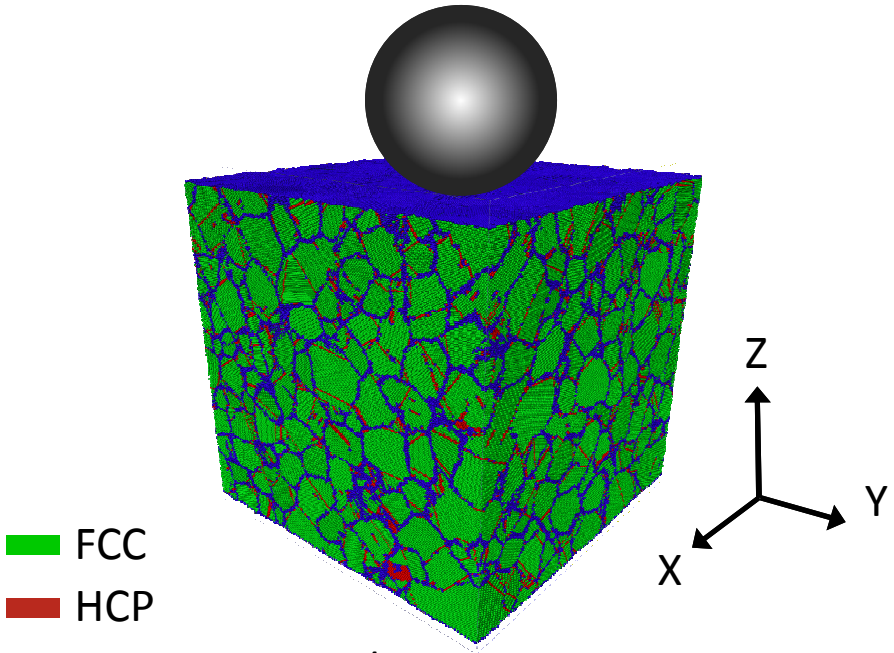

- Rigid atomic slab at bottom of film (0.6 nm)
- R=15 nm spherical indenter
- Repulsive potential:

$$F = K(r - R^2)$$

$$K = 10\frac{eV}{\mathring{A}^3} = 1.6\frac{\mu N}{nm^2}$$

- Constant velocity indentation:
  - 0.2 m/s, 1.0 m/s, and 5.0 m/s
- Three phases:
  - Indentation, hold, and removal of indenter.

Tucker and Foiles, Materials Science and Engineering A 571, 207 (2013)

Sandia National Laboratories

Computational Methodology – Indentation History

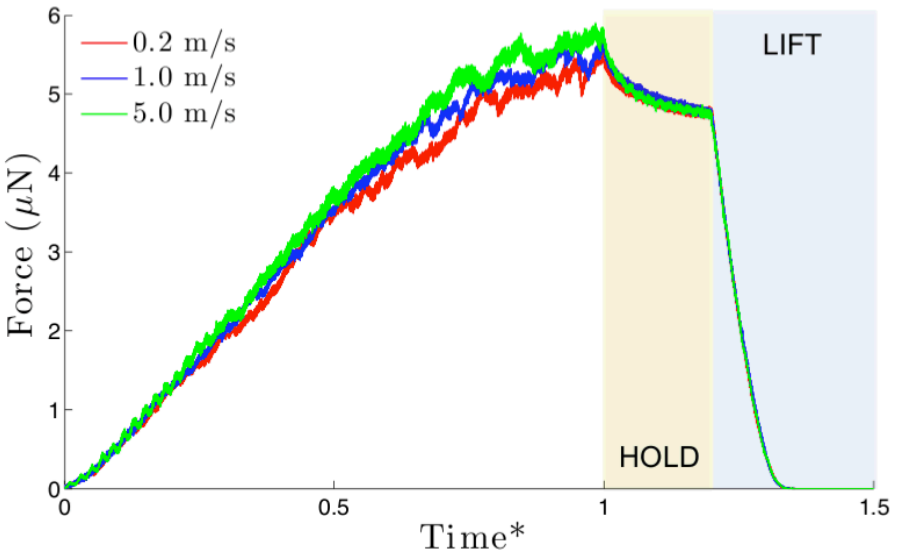

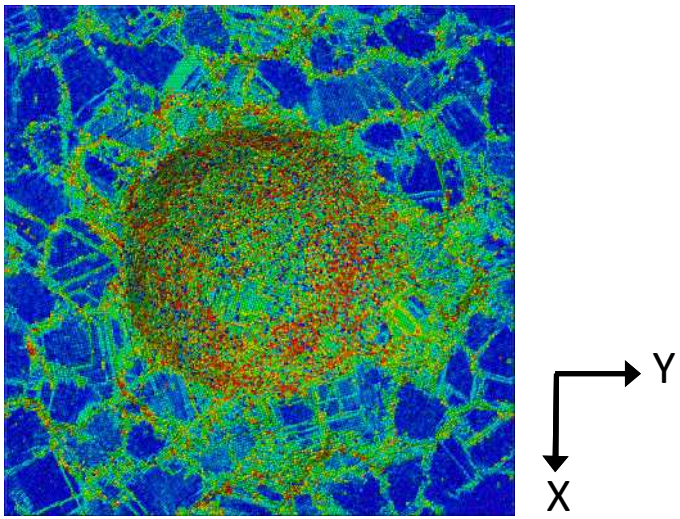

- Rigid atomic slab at bottom of film (0.6 nm)
- R=15 nm spherical indenter
- Repulsive potential:

$$F = K(r - R^2)$$

$$K = 10\frac{eV}{\mathring{A}^3} = 1.6\frac{\mu N}{nm^2}$$

- Constant velocity indentation:
  - 0.2 m/s, 1.0 m/s, and 5.0 m/s
- Three phases:
  - Indentation, hold, and removal of indenter.

- Simulation results show that the force on the indenter is rate-dependent - greatest for the highest indentation rate (5.0 m/s).
- The normalized relaxation rate during the 'hold' and 'lift' phases is approximately identical for all three indentation rates.

Tucker and Foiles, Materials Science and Engineering A 571, 207 (2013)

Sandia National Laboratories

Individual grains can be identified and tracked

To separate individual grains:

- Must designate the atomic crystal structure – Common Neighbor Analysis (CNA)
  - FCC, HCP, BCC, and other
- Compute the neighbor list of every atom based on a user-defined cutoff distance, r_{cut} (3^{rd} nearest neighbors are used in this work)
- Compute the concentration of FCC atoms around every atom based on the neighbor list.
  - *Ignore HCP neighbor atoms from criteria*
- If all neighbor atoms are FCC -> 'Grain-center'
- If some neighbors are not FCC -> 'Grain-edge'
- Loop over 'Grain-center' atoms and group into clusters based on neighbor lists and cutoff.

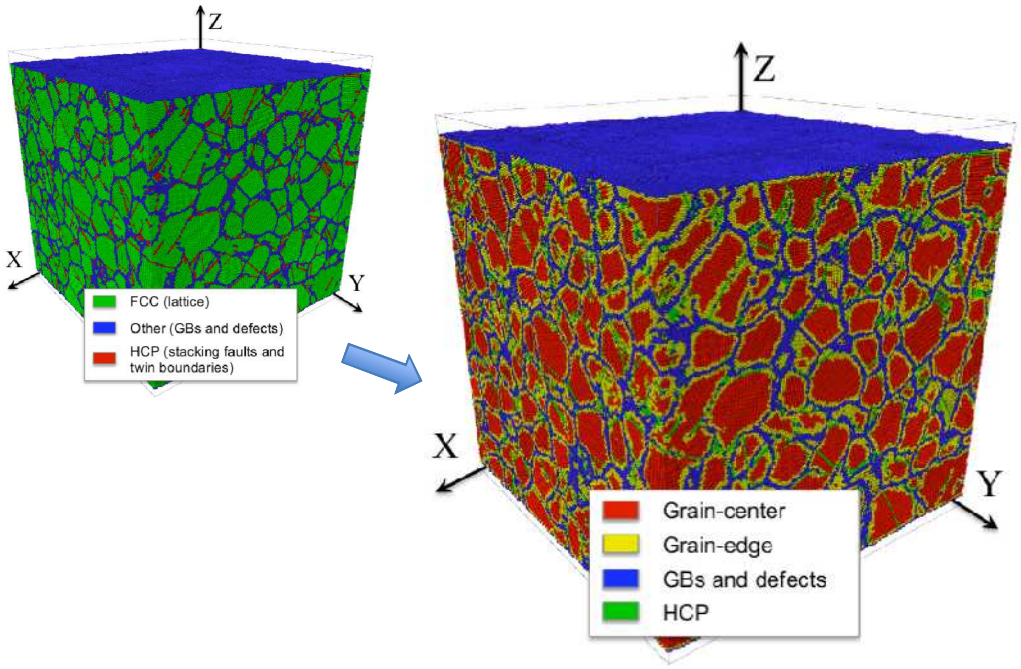

⟶ We know which atoms are in each grain

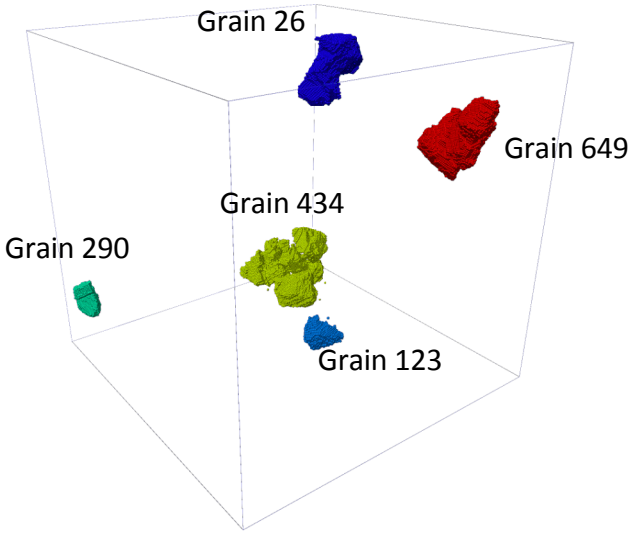

Now, we can distinguish individual grains from each other, compute microstructural evolution, and estimate metric changes as a function of indentation and imposed strain.

Tucker and Foiles, Materials Science and Engineering A 571, 207 (2013)

Analysis can track evolution of grain boundary area and the motion of grains

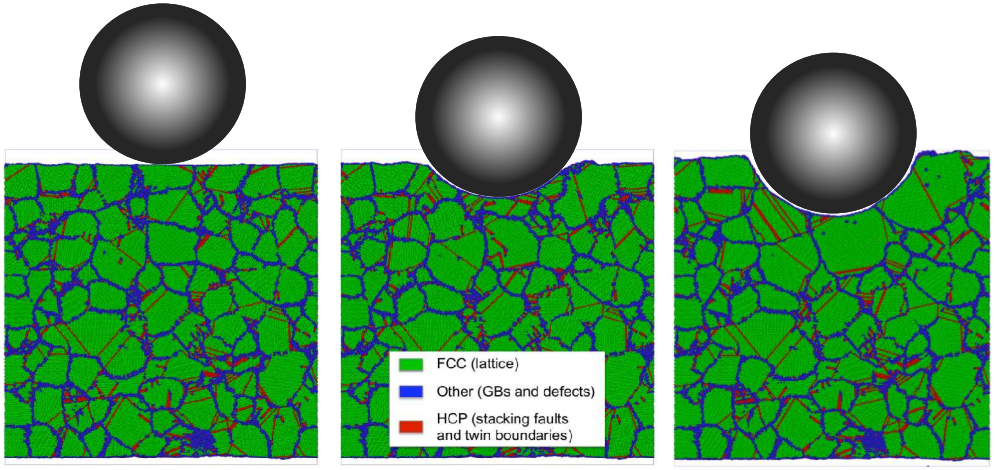

Comparison of initial and final states provides shows the elimination of grain boundaries near the indenter

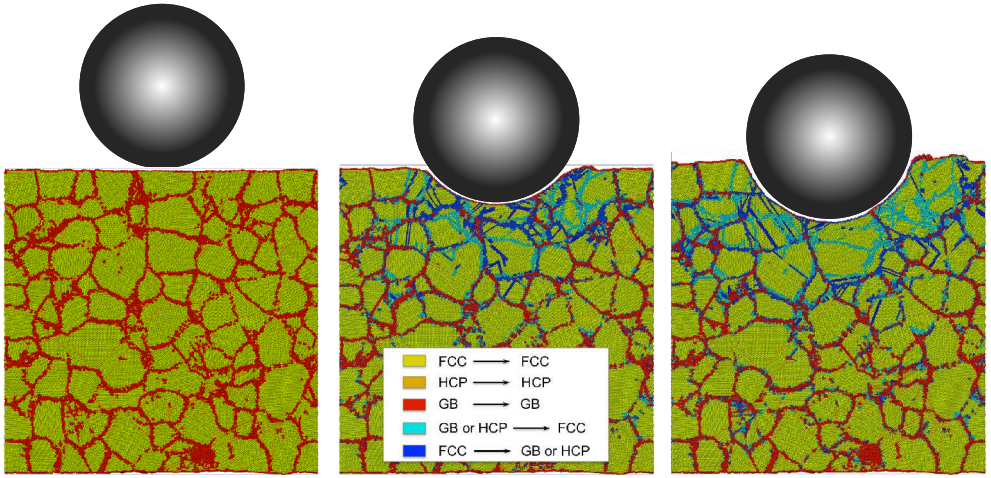

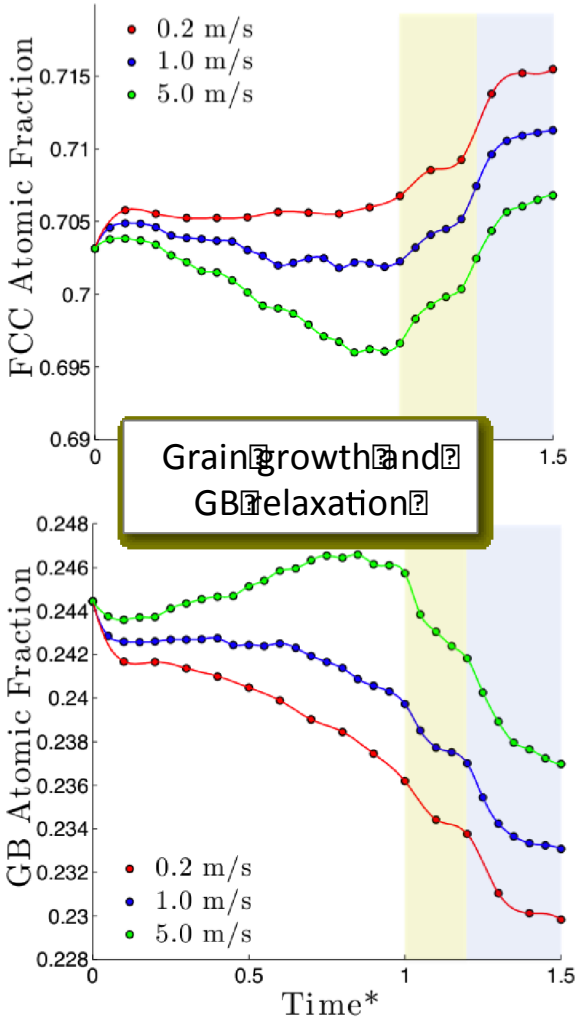

Significant rate dependence in the evolution of grain boundary area

Tucker and Foiles (2012), Mat. Sci. Eng. A, in press

Sandia National Laboratories

Grain growth enhanced at slower indentation rates

By comparing the Total Volume of each grain size at the end of the simulation, our results show that in general, **a slower indentation rate leads to more grain growth**.

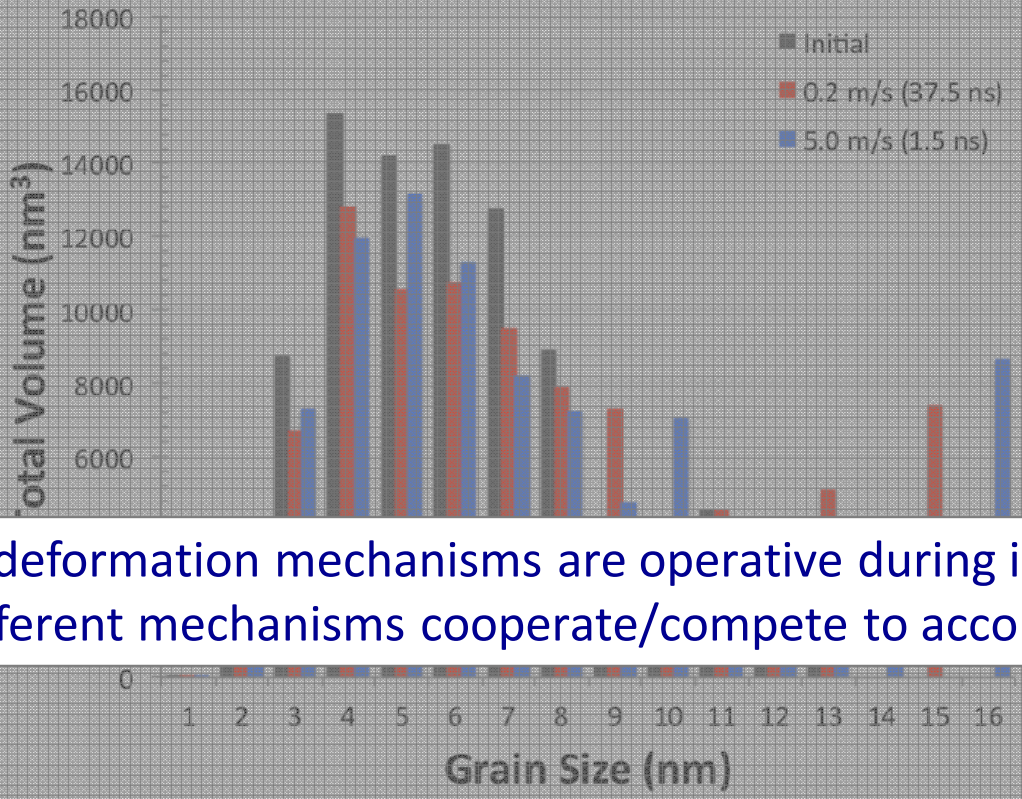

What deformation mechanisms are operative during indentation?
How do different mechanisms cooperate/compete to accommodate strain?

Combination of analysis methods reveals the dislocation and twin boundary evolution

- Utilize neighbor lists and computed metrics to determine atomic slip and local neighborhood.

Slip Vector $$s^{\alpha} = -\frac{1}{n_s}\sum_{\beta \neq \alpha}^{n}(x^{\alpha\beta} - X^{\alpha\beta})$$

- Assign non-GB atoms integer values for deformation mechanism group
  - Dislocations (Partial/Full)
  - TBs

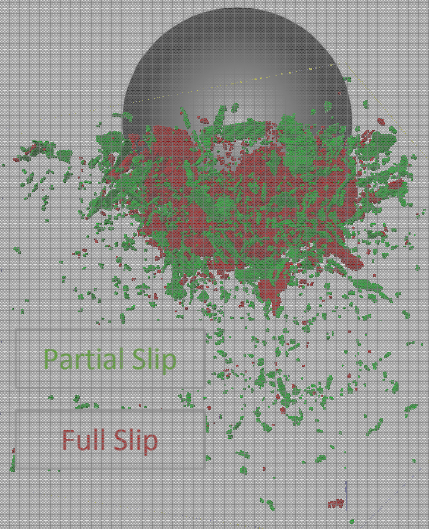

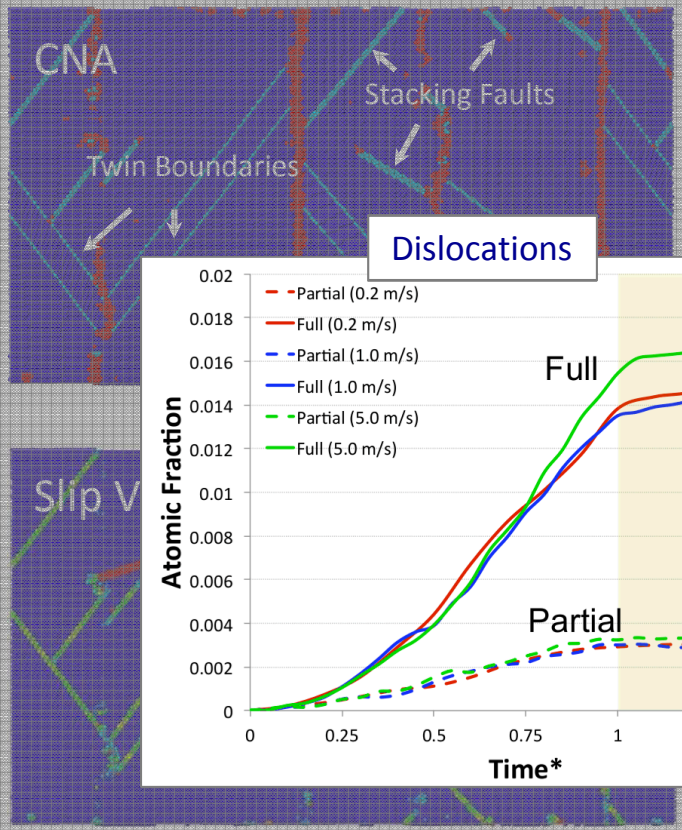

Dislocations

Twin Boundaries

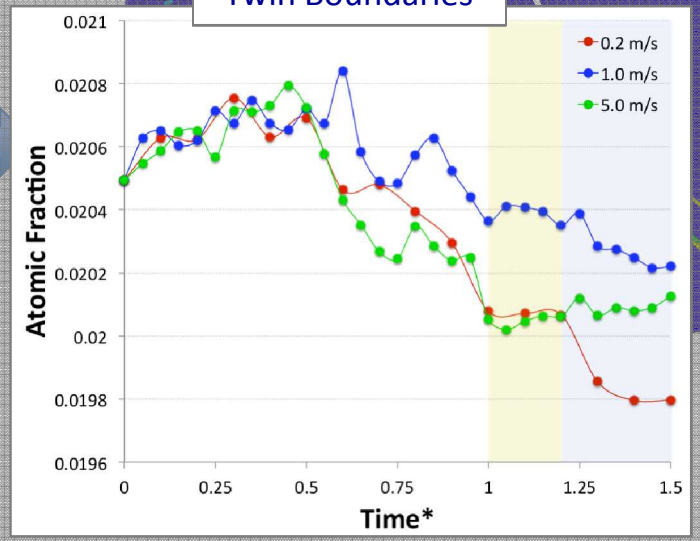

Strain Accommodation is Localized to Interfaces and Dislocations

Deformation Gradient Tensor $F_{iI}^{\alpha} = \omega_{iM}^{\alpha}(\eta^{\alpha})_{MI}^{-1}$

Green Strain Tensor $\boldsymbol{E} = \frac{1}{2}(\boldsymbol{F}^{\boldsymbol{T}} \cdot \boldsymbol{F} - \boldsymbol{I})$

- *tr*(E) from all atoms in a phase (e.g. FCC, GB, Dislocation) added together.
- Strain accommodation from Interface plasticity is substantial
  - Some relaxation during release
- Dislocation plasticity is roughly rate-independent and does not relax during release

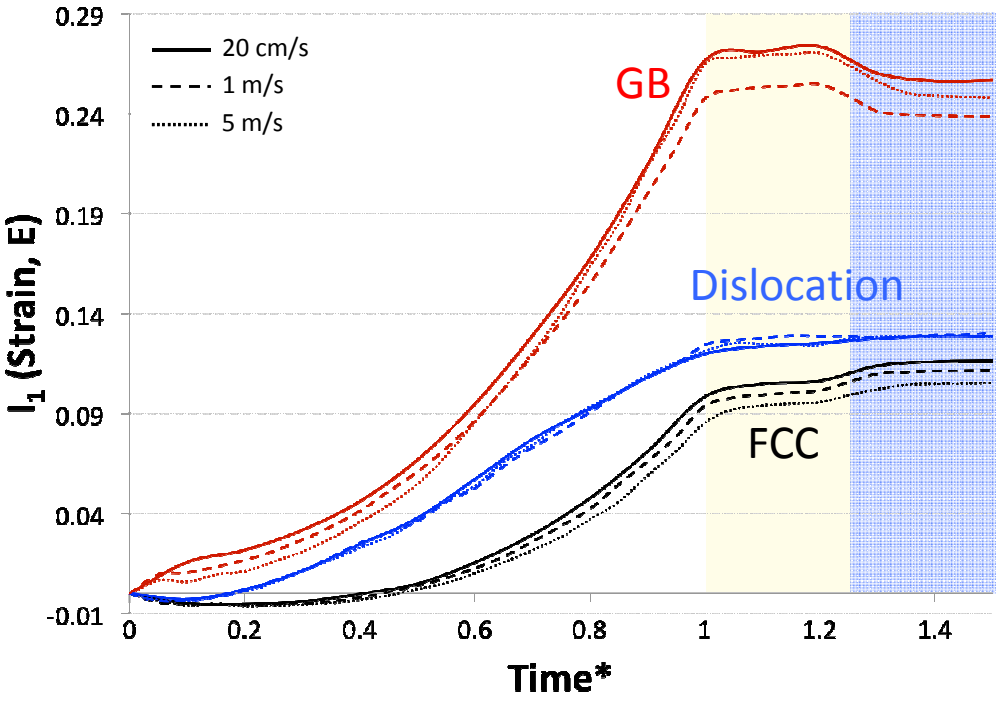

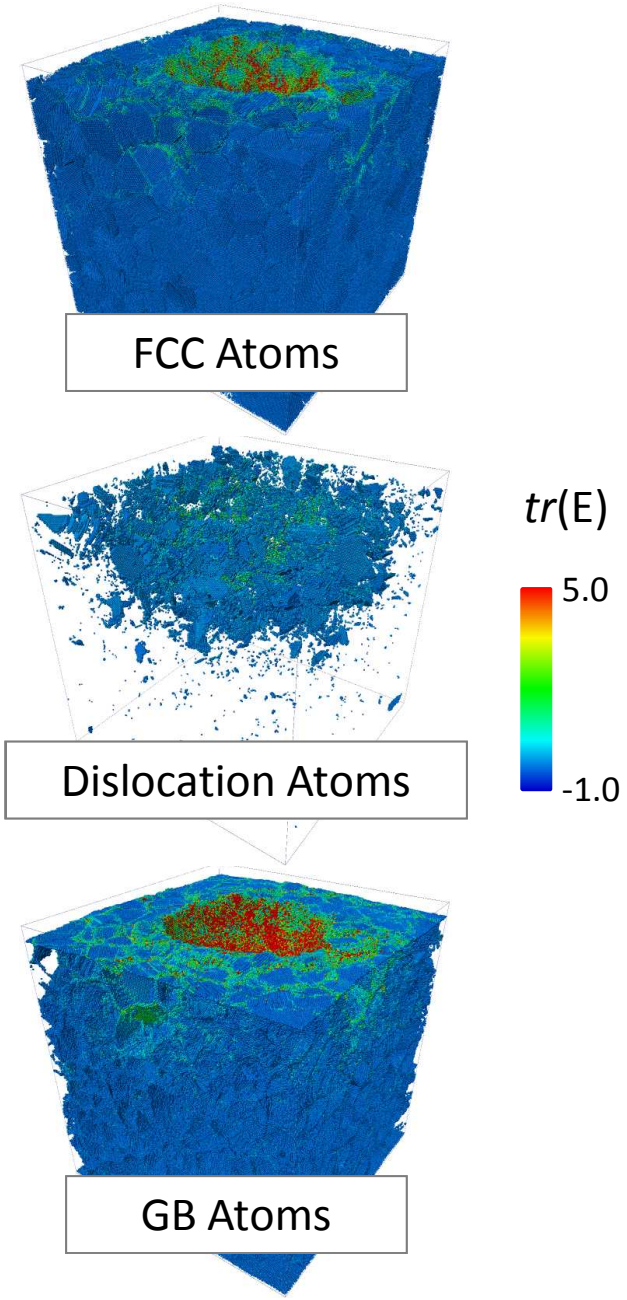

Outline
4 short case studies for microstructural evolution

- Pass information to meso-scale grain growth models
  - Grain Boundary Energies
    - Five-degrees of freedom challenge
    - Comparison with experimental observations
  - Grain Boundary Mobilities
    - Methodlogy
    - It is a lot more complicated than typically though
- Brute-force simulations of grain evolution
  - Annealing of nanocrystalline grain structure
    - Comparison of growth kinetics to conventional models
  - Nano-indentation of nanocrystalline metals
    - Deformation induces grain growth?
    - Identification of deformation mechanisms

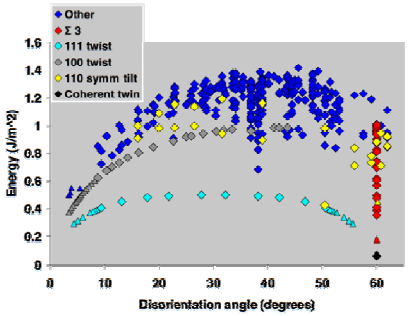

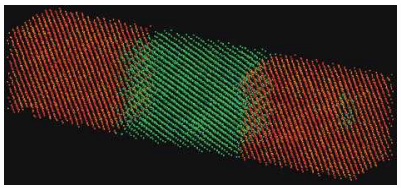

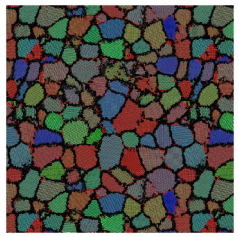

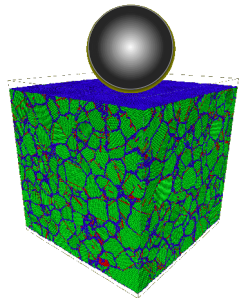

Sandia National Laboratories

Supplemental Slides

What is the big deal about determining grain boundary properties?

- *"We hold these truths to be self-evident, that all grain boundaries are NOT created equal, that they are endowed by their material with certain fundamental properties, that among these are Energy, Mobility and Deformation Response…"*
  - apologies to Thomas Jefferson
  - There is a **5-dimensional** space of macroscopic grain boundary structure
  - Energy and mobility vary throughout this 5-D space in an, at best, partially understood manner
  - And this doesn't even consider the effects of impurities, precipitates, …

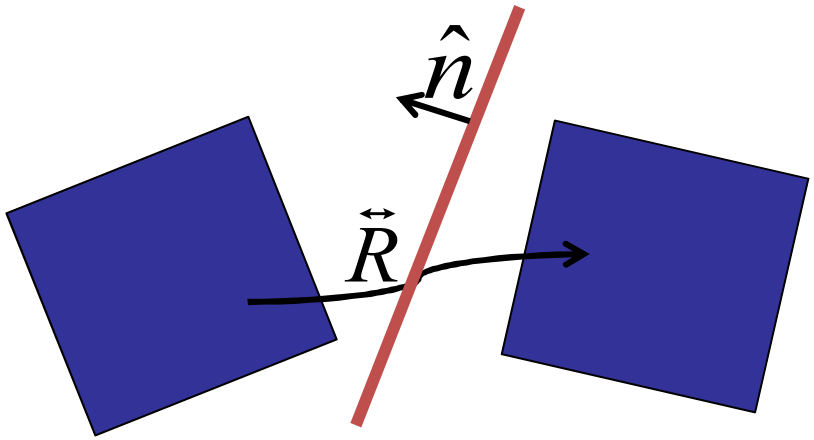

Sandia National Laboratories

Feeding mesoscale simulations of micrsostructural evolution with interfacial property data

- Consider two nearly identical grain growth simulations:

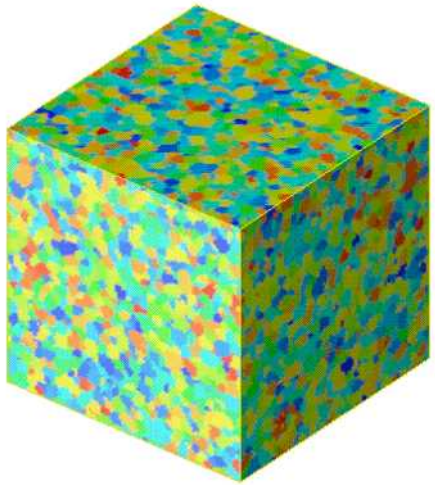

Uniform boundary energy and mobility → uniform grain growth

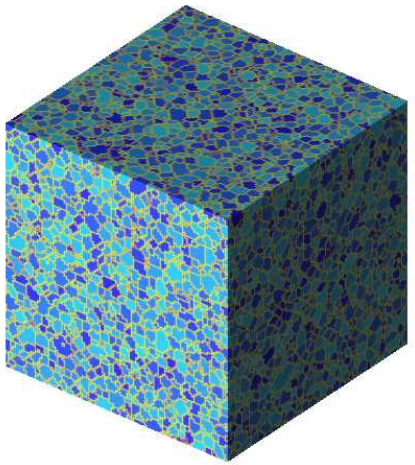

Uniform boundary energy and misorientation-dependent mobility → highly nonuniform grain growth

- The only difference between these simulations is a grain boundary mobility function that depends on crystallography.

⇒**In order to accurately model microstructural evolution, we need accurate values for boundary properties.**

Sandia National Laboratories

The relationship between grain boundary population and grain boundary energy

- Both theory and experiments suggest the GBCD (population) is related to the boundary energy: $\ln(P) \propto \gamma$
- The correlation between measured $\ln(P)$ and calculated γ is stronger than that between measured and calculated energies.
- The GBCD is a more direct and accurate representation of the microstructure.

⇒The grain boundary population provides a more robust metric for comparison to calculated grain boundary energies.

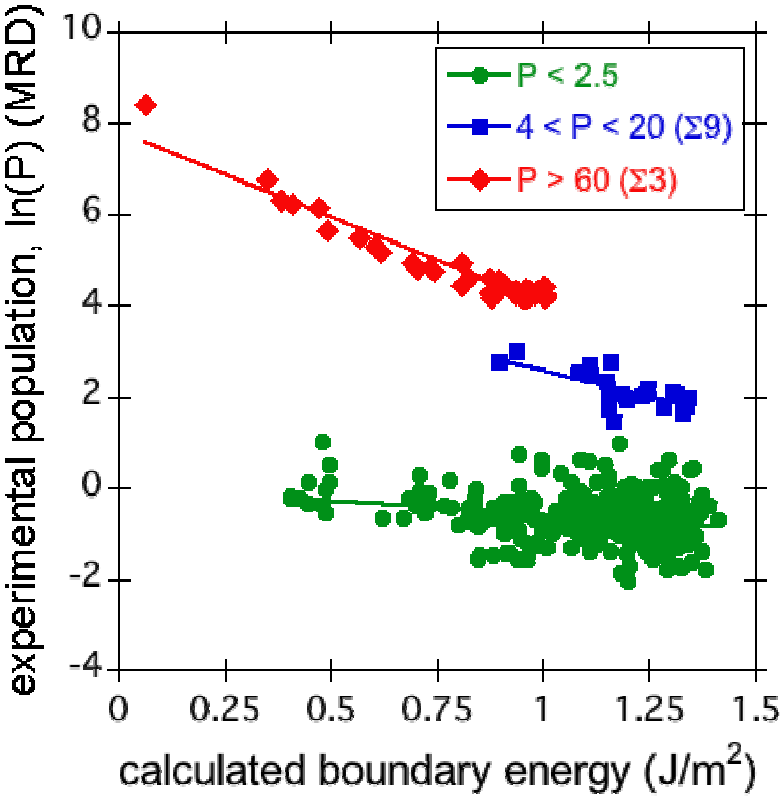

[Rohrer *et al.*, *Acta Mater.* **58** 5063 (2010)]

Sandia National Laboratories

Validating additional grain boundary types: Low stacking fault materials

- Ni microstructures are dominated by the twin network, comprised mainly of $\Sigma 3$ and $\Sigma 9$ boundaries.
- In Ni, only the $\Sigma 3$ and $\Sigma 9$ boundaries were observed in sufficient populations to compare to simulation data.
- Higher stacking fault materials such as Al should contain fewer twins, permitting additional boundary types to be observed.

$\Rightarrow$We investigate the GBCD of a large Al polycrystal.

- Commercially pure Al alloy 1050
- ~77,000 grain boundaries
- Characterized by EBSD and stereological analysis

Computation vs. experiment in Al: Complete boundary set

- As in Ni, the population-weighted correlation shows excellent agreement between experiment and simulation: $R_W \sim 0.91$.
- Also as in Ni, agreement is stronger for higher population boundaries.
- The 50.6°[111](111) boundary has higher population than predicted due to overlap with the coherent twin bin.
- The Σ11 50.5°[110](311) outlier is unexplained.

⇒Experimental results in Al validate computational data, as in Ni.

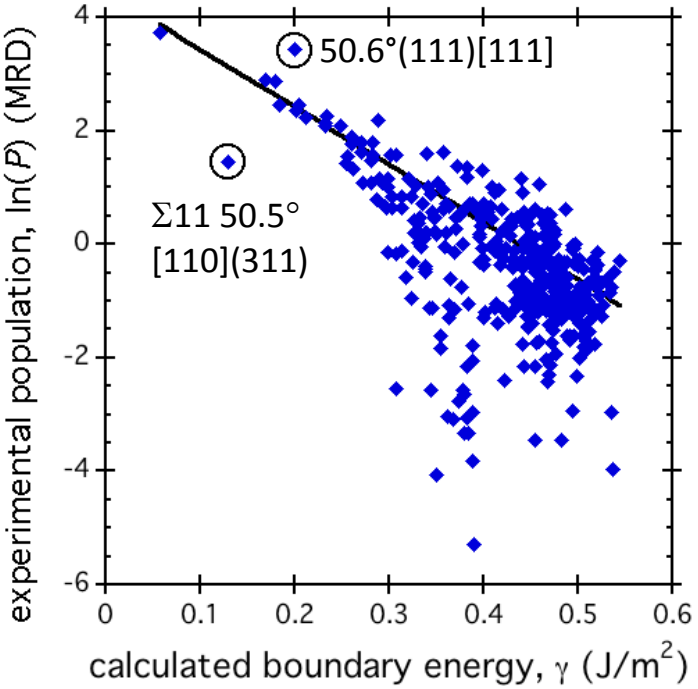

Sandia National Laboratories

Different grain sizes evolve differently during the indentation

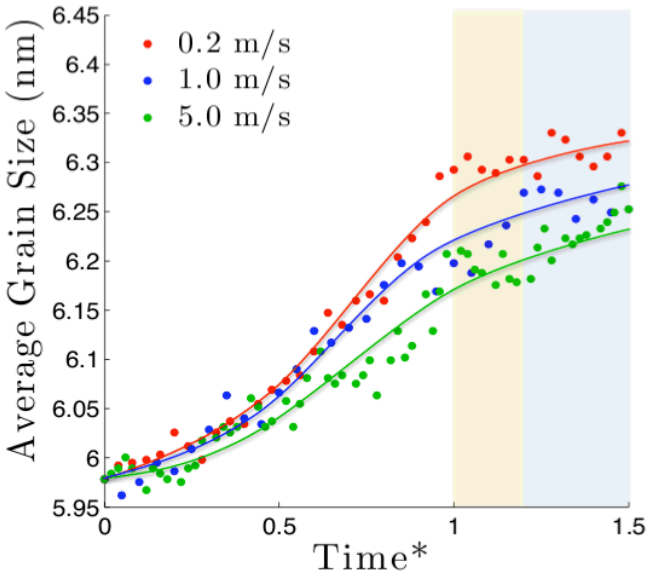

Average grain size increases slightly during grain growth and shows a dependence on the applied indentation rate

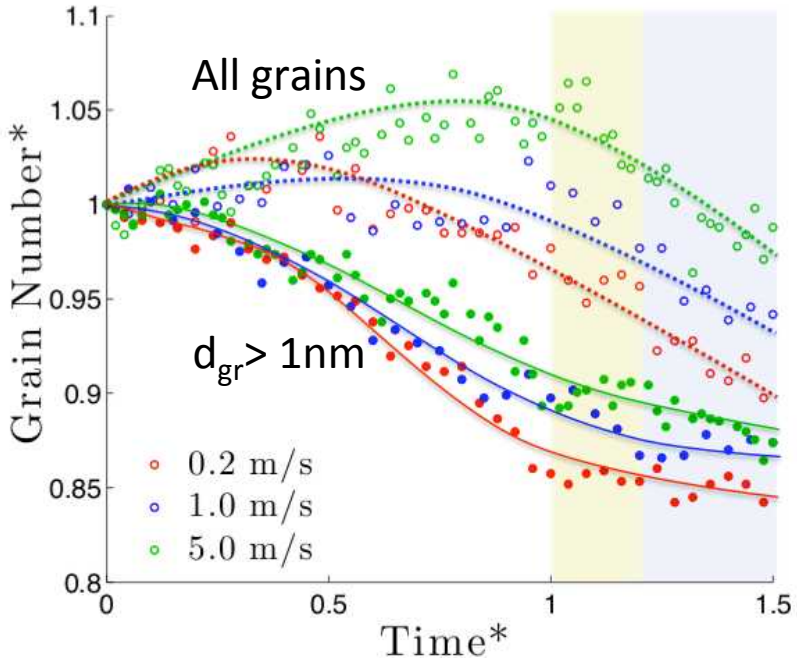

- Total number of grains increases during indentation and drops during hold and release
  - Driven by formation of small grains during indent
- However, for significant grains (d_{gr} > 1nm), grain growth grain growth occurs during indentation and slows during hold and release
- For both behaviors, there is modest rate-dependence in the observed grain growth trends.

Tucker and Foiles (2012), Mat. Sci. Eng. A, in press

Microscale Kinematic Metric Formulation reveal local deformation modes

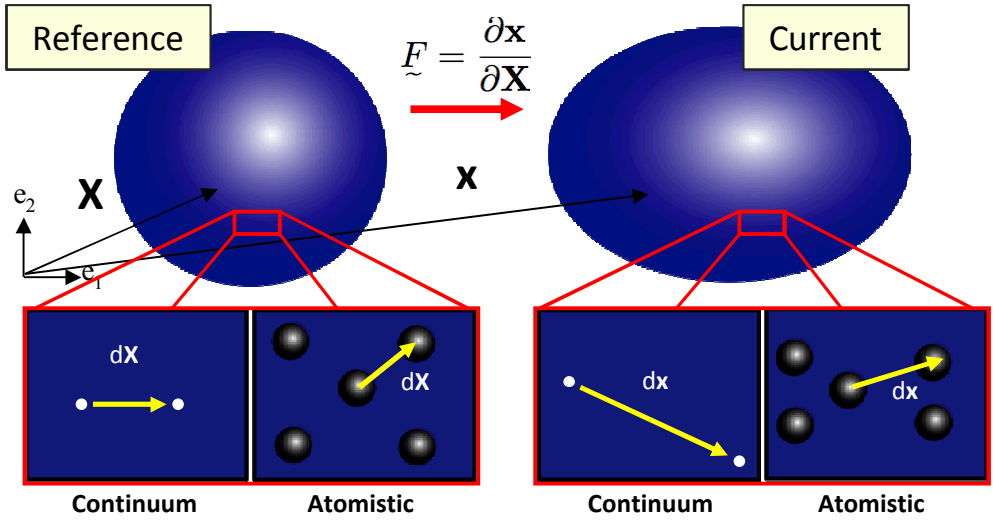

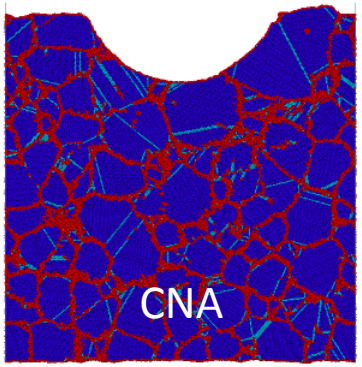

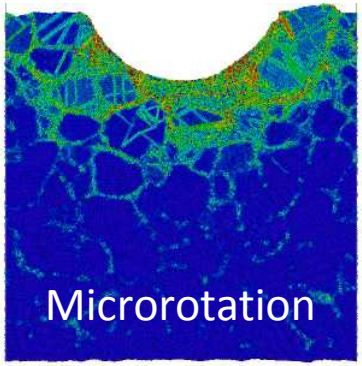

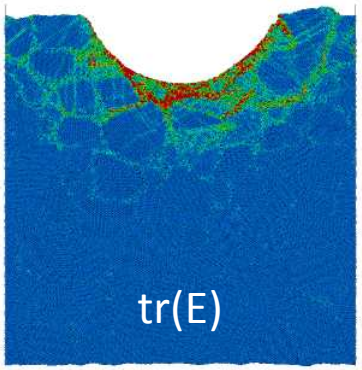

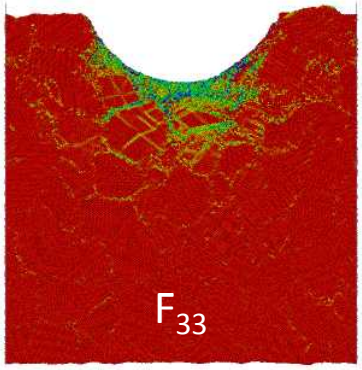

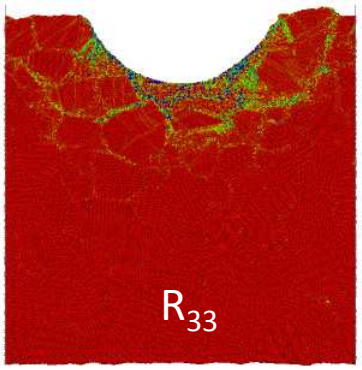

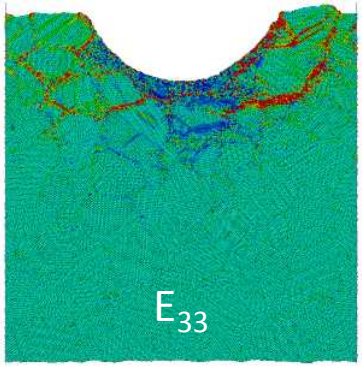

Deformation Gradient

$$F = \frac{\partial x}{\partial X} \rightarrow \sum_{\beta=1}^{n}(x_i^{\alpha\beta}X_M^{\alpha\beta} - F_{iI}^{\alpha}X_I^{\alpha\beta}X_M^{\alpha\beta}) \quad 0 \rightarrow \boxed{F_{iI}^{\alpha} = \omega_{iM}^{\alpha}\left(\eta^{\alpha}\right)_{MI}^{-1}}$$

where $\omega_{iM}^{\alpha} = \sum_{\beta=1}^{n} x_i^{\alpha\beta}X_M^{\alpha\beta}$

and $n_{iM}^{\alpha} = \sum_{\beta=1}^{n} X_I^{\alpha\beta}X_M^{\alpha\beta}$

Microrotation

$$\underset{\sim}{F} = \underset{\sim}{R}\underset{\sim}{U} \text{ where } \underset{\sim}{R} = \underset{\sim}{R}_{sym} + \underset{\sim}{R}_{skew} \rightarrow \underset{\sim}{R}_{skew} = \frac{1}{2}(\underset{\sim}{R} - \underset{\sim}{R}^{T}) \rightarrow \boxed{\phi_k = -\frac{1}{2}\varepsilon_{ijk}\left(R_{skew}\right)_{ij}}$$

Green Strain

$$\boxed{\mathbf{E} = \frac{1}{2}(\mathbf{F}^{\mathrm{T}} \cdot \mathbf{F} - \mathbf{I})} \quad \text{and} \quad I_1(E) = tr(E)$$

Zimmerman et al., IJSS (2009)
Tucker et al., MSMSE (2010)
Tucker et al., JMPS (2012)